Chapter 14
Nanoparticles for Cleaning up Oil Sands Process-Affected Water

Afif Hethnawi, Adle Mosleh, and Nashaat N. Nassar

14.1 Introduction

With industrial development, energy demand from conventional and renewable energy sources increases and becomes crucial concern [1]. Renewable sources of energy, despite their general awareness, are contributed only about 19.1 % of the global energy demand in 2013 [2]. Up to date, this trend has been growing steadily [3]. Thus, fossil fuel obtained by conventional crude oil stands out to remain the predominant energy source worldwide for the upcoming decades [4]. This demand, as reported by the International Energy Agency (IEA), is expected to rise from 84.7 million barrel/day in 2008 to 105 barrel/day in 2030 [5, 6]. However, the conventional reserves of oil are depleting [6, 7]. Thus, more efforts are needed to shift the oil production from conventional to the development of nonconventional resources, including oil sands [6]. The conventional oil reserves are more economically feasible to recover and process compared with that for the unconventional oil reserves [4, 7, 8]. Canada, for instance, is ranked as third globally (along with Saudi Arabia and Venezuela) in terms of domestic oil reserves [9]. The reserves in northern Alberta, Canada, are estimated to contain more than 1.7 trillion barrels of bitumen, as a largest oil deposits in the world [3]. For that reason, oil industry is considered and an energy intensive industry and a major consumer for the fresh water. This led such industry to be subjected to strict environment regulations, and hence, the oil industry is considering improving the efficiency and reducing the environment footprint of current oil recovery, storage, and pipeline transportation methods.. In terms of recovery, the deposited oil or bitumen, depending on how deep the oil sands reserves,

A. Hethnawi · A. Mosleh · N. N. Nassar (✉)
Department of Chemical and Petroleum Engineering, University of Calgary, Calgary, Alberta, Canada
e-mail: nassar@ucalgary.ca

N. N. Nassar et al. (eds.), *Nanoparticles: An Emerging Technology for Oil Production and Processing Applications*, Lecture Notes in Nanoscale Science and Technology, https://doi.org/10.1007/978-3-319-12051-5_14

is essentially recovered by employment of two main methods: open-pit mining or in situ extraction methods that are schematically shown in Fig. 14.1.

Less than 20 % of Alberta's bitumen reserves are close to the surface to be mined (less than 50 m) [3]. Anything deeper cannot be economically mined because huge amount of waste material needs to be removed before accessing to the bitumen-rich oil sands [9]. For about 80 % of Alberta's oil sands (deeper than 50 m), in situ thermal method can be used with substantial consumption of energy and water [9].

Unlike surface mining, in situ technology offers the benefit of removing the bitumen from the ground while leaving the sand in place [9]. Typically, an average of 0.4 barrels of fresh water is needed to recover each barrel of bitumen by SAGD process, while oil sands surface mining process uses three to four barrels of high-quality water for each barrel of oil produced [10, 11]. In Alberta, most of the high-quality water (around 90%) used for mining operations is typically recycled from the production process, while the rest is withdrawn from the Athabasca river [10,

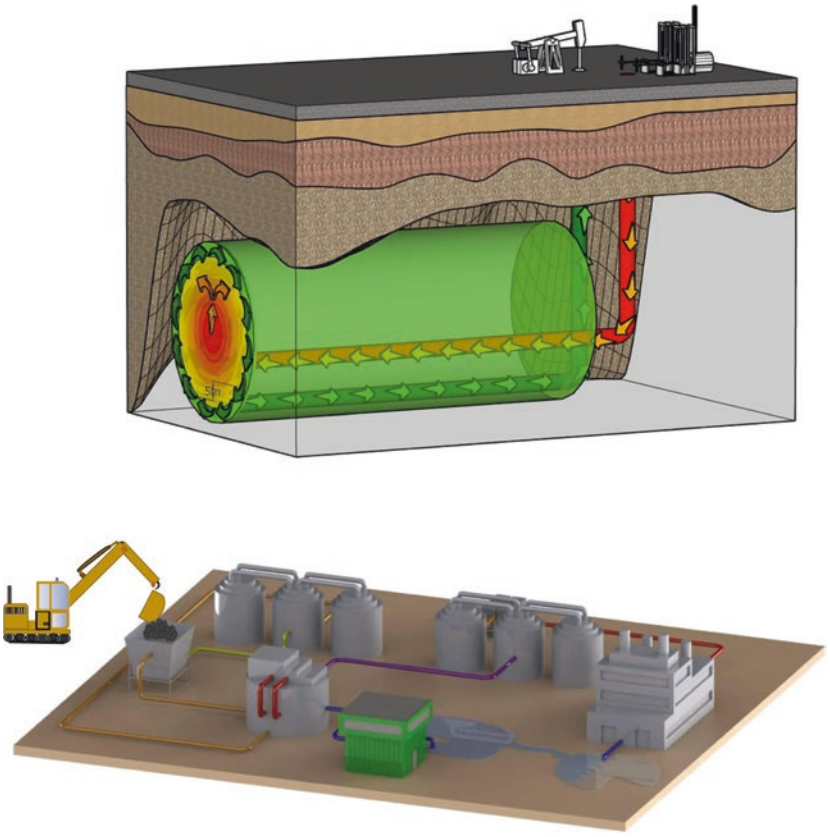

Fig. 14.1 Schematic representation for the extraction of bitumen from oil sand through (**a**) steam-assisted gravity drainage (SAGD) and (**b**)open-pit surface mining processes. Copyright permission was obtained from Vista Projects (https://www.vistaprojects.com/)

11]. The most well-known in situ process is SAGD which is currently considered as the most widely practiced one for bitumen extraction from oil sands in Alberta, Canada, due to its lower cost and higher efficiency. In Alberta alone, 80% (or 135 billion barrels) of the oil sands are located in these underground deposits and would be difficult to access without applying SAGD process [12]. In principle, SAGD process requires drilling of two horizontal wells [13–15]. The upper well is utilized to inject the heated steam inside the oil well deposit [13–15]. This steam builds up heat, which delivers its latent heat to the adjacent area, reducing the viscosity of the bitumen and subsequently mobilizing it [13–15]. Thus, the mobilized bitumen, along with the condensate steam, is drained downward by gravity to the second horizontal well, from which it pumps to the surface [13–15]. The recovered bitumen on the surface is separated via subsequent cooling units, generating huge amounts of wastewater in the form of produced water (PW). Then, the bitumen is transferred to surface-upgrading facilities in order to convert the low-quality oil to synthetic crude oil. The PW, on the other hand, is transferred to sequential de-oiling and treatment train to improve the water quality to be reused for boiler feedwater (BFW) in a once-through steam generator (OTSG) that produces steam from a high-quality water [9, 12, 16]. Constrains on water quality are produced by once-through steam generator (OTSG). OTSG is specifically developed heat recovery steam generator for thermal recovery applications [17]. In OTSG design, a single pass of water through the generator coil and no separator drum are available, generating 80 % quality steam with water-to-steam ratio of 1:4 [3]. PW is generally characterized by having high concentrations (from 1000 to 10,000 mg/L) of brine, silica, alkalines, and total dissolved solids (TDS) [18–20]. Exceeding the "threshold requirement concentrations" is undesirable for the reuse of PW as boiler feedwater (in oil field steam generator), unless it can be effectively treated through selective water treatment technologies [21]. Thus, the generated SAGD produced water must meet the strict requirements in the employed boiler for steam generation [17, 22–25]; otherwise, boiler drum and tubes can be damaged or corroded.

On the other hand, open-pit mining, like traditional mineral mining operations, is largely employed where oil sands reserves are closer to the surface [26]. Practically, large shovels scoop the oil sand into trucks which then move it to crushers where the large clumps of earth are processed [26, 27]. Then, the crushed oil is mixed with warm water, oil sand lumps and rocks, air, and caustics, forming slurry mixture that mainly composed of about sand with minimal composition of bitumen [26, 27]. After that, the slurry mixture undergoes to a simple water-based gravity separation process to extract the bitumen fraction [26–28]. In the gravity separation vessel, flotation cells are used to liberate the bitumen deposited in the sand grains by injecting free air bubbles to slurry mixture, generating a froth product that is formed on the top of the vessel [26–28]. This froth composes of about 60% by weight bitumen, 30% water, and 10% solids [26–28]. The unrecyclable effluent is discharged to tailing ponds [26–28]. The bitumen froth is further treated with organic solvents to remove water and residual solids from the bitumen, before sending it to upgrading plants [26–28]. The bottom product is mostly composed of solids and water in the form of tailings and is pumped to tailing ponds. In those tailing ponds, the mixture, based on the sand

particle size and compositions, is separated into two main layers: a layer of coarse solids with characteristic size greater than 44μm and other layer enriched with smaller fine solid particles [29]. The heavier layer tends to be settled down at high rate and precipitate quickly to be used to construct contaminant dikes, while the other layer remains at the top of the pond as fluid fine tailings [26–29]. From the fluid fine tailings, great portion of fine sand particles and clay stay suspended and eventually form a mud-like slurry (30–45% solids by weight) called mature fine tailings (MFT) [26–29]. Around 86% of the volume of MFT contains water that cannot be easily recycled, because of the presence of stable sand particles (very fine, negatively charged clays that cannot be separated from water by gravity); these sand particles form a vastly disproportional amount of slurries that constantly repel each other, inhibiting Brownian agglomeration and making it difficult for settling to take place [26–29]. To address this challenging issue, tremendous efforts, with varying levels of success and feasibility, have been proposed to speed up the settling rate of the fine particles in MFT and maximize the water recovery rate [29].

With respect to storage and transportation of the recovered oil, pipelines are a critical part of Canada's oil transportation infrastructure [30, 31]. Pipeline transport is the safest and most efficient way to move large volumes of oil from development areas to refineries, petrochemical plants, and even to homes or businesses [30, 31]. Although pipelines are convenient and appear to be better options compared to other means of transportations, there are issues to be concerned like crude oil spills. For instance, the TransCanada pipeline that transports oil to the US Midwest has experienced 14 spills, with the latest spill at North Dakota pipeline pumping station in May 2011[30, 31]. A campaigner with Greenpeace Canada considers this as an act of aggression toward plants, wildlife, and people who live in the path of pipelines. In fact, these oil spills, without an effective removal method, showed adverse impacts to ecosystems and the long-term effects of environmental pollution that calls for an urgent need to develop a wide range of materials for cleaning up oil from oil-impacted areas [32].

In conclusion, bitumen recovery operations (i.e., open-pit mining or SAGD) and oil pipelines generate a considerable amount of oil sands process-affected water (OSPW) and oil spills. These OSPWs, without any treatment, can cause low bitumen recovery, fouling, corrosion, and scaling problems at the extraction and transportation facilities. As a result, a series of OSPW treatments is necessary before recycling or environmental release of this water. Therefore, oil sands companies in Canada are eagerly seeking novel technologies in order to modify the technologies they currently implement for recycling the generated OSPW. In this regard, this chapter aims to provide an overview about the main conventional treatment technologies applied in treating SAGD produced water, mature fine tailings (MFT), and oil spills. Thus, the chapter critically highlights and deeply describes the conventional treatment technologies along with their suggested modification methods and some emerging techniques that have been recently reported from fundamentals to process optimization and eventually the parameters that affect the process efficiency. The chapter comprehensively describes tailoring designs of some eco-friendly nanoparticles developed by Nassar's group at the University of Calgary to

be effectively combined or integrated with the many physical and/or chemical processes utilized for remediation of OSPW.

14.2 Treatment of SAGD Produced Water

During the SAGD operations, the strict water quality requirements for steam generation can be met by reducing the levels of suspended and dissolved organic matters, hardness, and silica [33]. For example, the level of TOC, which reflects soluble, emulsified, and suspended organics, in produced water varies from 100 to 700 ppm [21, 24, 33]. Also, silica levels can reach up to 400 ppm. These levels should be maintained below 50 ppm TOC and 30 ppm silica in the feedwater to OTSG [21, 24, 33]. Thus, sequential primary, secondary, and tertiary stages are conventionally applied. In the primary stage, the oil content is reduced from 2000 to 500 ppm from the PW by applying three-phase separators followed by skimming [15]. These separator units maintain high retention times (i.e., 3h), which allows for oil/water separation. In the primary stage, the suspended solid presented in the PW is removed by induced gas flotation (IGF) process that uses air or, low density gas, typically methane [15]. However, introducing gasses in IGF in some occasions cannot effectively remove the suspended solid and requires high retention times [15]. Therefore, ionic polyacrylamide is added to flocculate the suspended solids in the IGF, which are able to destabilize the suspended solids via surface neutralization and facilitate floc formation by interparticle bridging mechanism[15]. The outlet from IGF is fed to a sand filter, which contributes to lowering the suspended solid concentration between 30 and 40 ppm. The tertiary stage consists of chemical treatment train that is aimed at reducing the residual concentrations of silica, TOC, and total hardness from the PW to meet water specification for the OTSG [15, 21, 24, 33]. The chemical treatment train combines three successive processes of warm lime softening unit (WLS), followed by walnut shell filtration (WSF), and weak acid cationic exchanging unites (WAC).

14.2.1 Warm Lime Softening (WLS) Unit

In the WLS, the hardness (calcium and magnesium ions) and total alkalinity are removed by adding chemicals like lime ($Ca(OH)_2$), soda ash (Na_2CO_3), and caustic soda (NaOH). As a result, the concentrations of silica and hardness are diminished to values less than 50 mg/L and 50 mg/L as $CaCO_3$ at high temperature (65−85 °C), respectively [15, 21, 24, 33]. Fundamentally, the silica, under the aqueous conditions, exists in crystalline or amorphous forms [34]. There are various forms of crystalline silica, but the most abundant one is quartz, having a very low solubility in water, around 6 mg/L (as SiO_2) at 25 °C [34]. However, amorphous silica is more soluble in water with maximum solubility of 100–140 mg/L (as SiO_2) at 25 °C [34].

The amorphous silica can be essentially classified as dissolved, colloidal, and particulate silica [34]. Dissolved silica includes various silica species: monomers (Q^0), dimers (Q^1), trimers (Q^2), and polymeric silicic acid (Q^3) as shown in Fig. 14.2 [34]. As reported previously, the silica species are in transition among each other according to the medium pH and the presence of other ions [34–36]. With polymerization of silicic acid by condensation, a three-dimensional gel network of insoluble or colloidal silica (amorphous silica) is generated [34–36]. Hence, the presence of diverse forms of silica is considered to be "anomalous," indicating that the stability in terms of pH does not follow a certain trend [35, 36]. Hence, the formed silica at various medium pH can be presented on two domain states of silica: colloidal domain, which is insoluble and amorphous (polymerization), and mono-clear silicate. At medium's pH above 9 (pH of SAGD produced water), the concentration of mono-clear domain silica and other species is dominant in an aqueous condition [34–36].

The removal of hardness and silica in WLS is carried out by introducing lime ($Ca(OH)_2$), soda ash (Na_2CO_3), magnesium oxide (MgO), and sodium hydroxide (NaOH) to the generated PW, in which the soluble calcium and magnesium hardness convert to insoluble calcium carbonate and magnesium hydroxide that contribute in simultaneous precipitation of silica [15, 17, 21, 24, 33]. Firstly, the removal of carbonate hardness by lime is accomplished by one of the following reactions [15, 17, 21, 24, 33]:

$$Ca(HCO_3)_2 + Ca(OH)_2 \Rightarrow 2CaCO_3 \downarrow + 2H_2O \tag{14.1}$$

$$Mg(HCO_3)_2 + Ca(OH)_2 \Rightarrow CaCO_3 \downarrow + MgCO_3 + 2H_2O \tag{14.2}$$

$$MgCO_3 + Ca(OH)_2 \Rightarrow CaCO_3 \downarrow + Mg(OH)_2 \downarrow \tag{14.3}$$

$$Ca(HCO_3)_2 + 2NaOH + Ca^{2+} \Rightarrow 2CaCO_3 \downarrow + 2H_2O + 2Na^+ \tag{14.4}$$

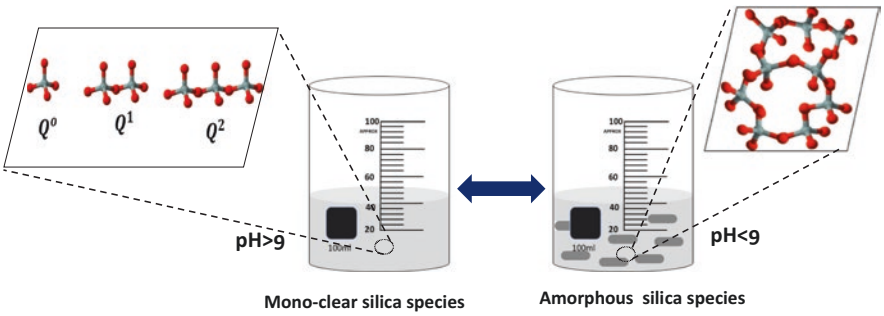

Fig. 14.2 Model of silica species and their polymerization path into amorphous structure under aqueous conditions. Color code: O: red; Si: light gray

Also, the removal of calcium non-carbonate hardness by soda ash is carried out by [15, 17, 21, 24, 33]:

$$CaSO_4 + Na_2CO_3 \Rightarrow CaCO_3 \downarrow + Na_2SO_4 \tag{14.5}$$

$$CaCl_2 + Na_2CO_3 \Rightarrow CaCO_3 \downarrow + 2NaCl \tag{14.6}$$

On the other hand, the removal of magnesium non-carbonate hardness by lime and soda ash can be done by one of the following chemical reactions [15, 17, 21, 24, 33]:

$$MgCl_2 + Ca(OH)_2 \Rightarrow Mg(OH)_2 \downarrow + CaCl_2 \tag{14.7}$$

$$CaCl_2 + Na_2CO_3 \Rightarrow CaCO_3 \downarrow + 2NaCl \tag{14.8}$$

$$MgSO_4 + Ca(OH)_2 \Rightarrow Mg(OH)_2 \downarrow + CaSO_4 \tag{14.9}$$

$$CaSO_4 + Na_2CO_3 \Rightarrow CaCO_3 \downarrow + Na_2SO_4 \tag{14.10}$$

With lime softening process, the silica presented in the PW can be significantly reduced via forming precipitated metal ions, such that the silica removal by magnesium oxide can be carried out in the same softening unit simultaneously with the removal of hardness from the PW by lime and soda ash [15, 17, 21, 24, 33]. Thus, the purpose of MgO addition is to interact with silica and precipitate silica compounds from the produced water. However, the mechanism at which the silica is removed by MgO has not been fully described [37–40]. Several studies based on physiochemical processes have investigated the removal of silica with the use of many metal oxide compounds [37–40]. Table 14.1 lists some attempts that have been reported to study the removal of silica by using different metal oxides/hydroxides from synthetic PW. The table includes the process involved in removing of silica in each study, materials used, summary of the main results, and references [37–40].

All the tabulated studies showed effective removal of silica through precipitation along with adsorption mechanisms using diverse metal oxides/hydroxides. It can be also noticed that the presence of MgO results in highly efficient silica removal, especially at high temperature (i.e., WLS conditions) [37–40]. In fact, using MgO after hydration at WLS conditions has shown faster and more efficient removal of silica. However, the MgO without sufficient hydration, which occurs in a separate slurry mixing tank, may exist in non-slaked form after reaching to the WLS unit, which contributes in attaining unpredictable performance in the real application. In fact, existence of non-slaked MgO at WLS conditions resulted in obtaining high removal of silica, compared with the slaked form, due to adsorption of silica on the surface of the formed $Mg(OH_{)2}$ [40]. Unfortunately, introducing great amount of magnesium compounds increases the conductivity in the treated waters, which can

Table 14.1 Most recent studies that have reported the removal of silica from synthetic produced water with the use of different metal oxides/hydroxides [37–41]

Process	Material and methods	Main results	References
Coagulation/ precipitation	Metal hydroxide (ferry, aluminum, and calcium)	The content of 35 mg/L SiO_2 in synthetic PW can be completely removed by aluminum compounds at ambient conditions.	[37]
		Aluminum compound as catalyzer reacts with colloid silica in the form of pure amorphism.	
		The soluble silica can be adsorbed by ferric hydroxide, which enhances the speed of colloid silica coagulation and settling at ambient conditions.	
		The concentration of soluble silica in treated wastewater is reduced to 3–5 mg/L when ferric coagulant is added.	
Coagulation/ flocculation	Combination of magnesium compound, sodium hydroxide precipitation, and zinc sulfate	The silica was removed at room conditions through magnesium compound, pH regulator, and zinc sulfate.	[38]
		The concentration of silica (calculated with SiO_2) was reduced to less than 50 mg/L in the optimal condition: 500–600 mg/L of NaOH, 700–800 mg/L of $MgCl_2{\cdot}6H_2O$, and 100–150 mg/L of zinc sulfate.	
		The removal efficiency of silica by zinc sulfate was higher than that by general coagulants such as aluminum and ferric salts.	
		High temperature (70–90EC) and long settle time (> 1.0 h) in a mixing jar were advantageous to the silica removal.	
Electroco agulation (EC)/ adsorption	EC by corrode Fe^0 or Al^0 anodes to release Fe(II) (or Al(III)) ions into the solution	Formation of Fe(II) or Al(III) allowed to react with solutes in the solution to form Fe-containing (or Al-containing) precipitates that can adsorb a wide variety of contaminants.	[39]
		In Fe^0-EC, the precipitation of FeS minerals resulted in a rapid removal of sulfide and adsorption of silica onto FeS.	
		In Al^0-EC, silica was removed via adsorption onto aluminum hydroxides, compared with sulfide that was poorly removed.	

(continued)

Table 14.1 (continued)

Process	Material and methods	Main results	References
Adsorption/ precipitation	Slaked and non-slaked MgO	Silica removal by slaked and non-slaked MgO has been investigated at different pH values (8.0−11.3) with different dosages (100−1000 ppm) and contact time (15−120 min) at WLS operating temperatures (65−85 °C).	[40]
		Silica removal takes place through two possible competing mechanisms: adsorption on the formed $Mg(OH)_2$ or precipitation by forming magnesium silicate precipitates.	
		Slaked MgO achieves lower silica removal percentage than non-slaked MgO at WLS conditions because MgO slaking makes silica adsorption on the formed $Mg(OH_)_2$ more predominant.	
Adsorption/ precipitation	Sparingly soluble magnesium compounds (MgO,$Mg(OH)_2$ and $(MgCO_3)_4{\cdot}Mg(OH)_2{\cdot}5H_2O$)	The use of three sparingly soluble magnesium compounds (MgO, $Mg(OH)_2$ and$(MgCO_3)_4{\cdot}Mg(OH)_2{\cdot}5H_2O$) has been investigated at three pHs (10.5, 11.0, and 11.5) and five dosages (250–1500 mg/L) at ambient temperature (~20 °C).	[41]
		The results showed that only 40% silica removal was obtained.	
		To increase silica removal, the slurries of sparingly soluble compounds were pre-acidified with concentrated sulfuric acid and tested at the same conditions. In this case, high removal rates were obtained (80–86%) at high pH (11.5), even at ambient temperature.	

be avoided by applying sparingly soluble magnesium compounds, such as (MgO,$Mg(OH)_2$ and $(MgCO_3)_4{\cdot}Mg(OH)_2{\cdot}5H_2O$)) that might be considered as promising alternative [41]. As a matter of fact, significant reduction in the conductivity was obtained by applying the sparingly soluble magnesium compounds, with low removal efficiency of silica (i.e., 40 %) at pH 10.5, dosages of 250 mg/L, and at ambient temperature (~20 °C) [41]. The same study showed that the removal efficiency of silica was then improved up to 80% by pre-acidifying the sparingly magnesium compounds with concentrated sulfuric acid, which is not industrially favorable [41].

From the listed studies in Table 14.1, it can be also noticed that all the suggested metal oxides/hydroxides applied to remove silica from organic-free synthetic produced water under conditions mimicking the WLS operations [37–41]. These results cannot be representative for the real performance of MgO in removing of silica from the authentic water, likely due to the influence of organic species. In addition, using massive amounts of lime, ash, and metal oxides/hydroxides for simultaneous removal of hardness and silica is costly ineffective, such that WLS contributes in 80% of the operation cost and 30% of the capital investment of the tertiary treatment train for the PW generated from SAGD process. In fact, introducing lime, ash, and slaked and non-slaked magnesium might enhance the concentration of divalent ions (i.e., Ca^{+2} and Mg^{+2}), which increase the need for another unit to be eliminated (i.e., WAC). Installation of WAC unit adds extra operational and capital costs for the whole chemical treatment process [17].

14.2.2 Walnut Shell Filter (WSF) Unit

In WSF, a deep bed-filter media, commonly termed walnut shell filters, are traditionally utilized due to their oil and solid filtration performance combined with ease of backwashing. WSF is applied to reduce the free oil content in SAGD produced water below 50 mg/L [17]. Practically, the walnut shell filter media, compared with other minerals and polymers, have several unique characteristics (e.g., hard, lightweight, chemically inert, nontoxic, and biodegradable) [42–45]. These characteristics, in addition to its high affinity to uptake many mineral oils and heavy metals, have motivated many industries to use them as effective filtration media or even active sorbents [42–45]. However, the walnut shell particles (WS-VR) have amorphous and compact structure due to high contents of cellulose and hemicellulose inert layers. Presence of such inert layer on the WS-VR, without surface modification, does not allow for enhancing the surface activity, thereby creating active sorbent that is able to capture many contaminants [42–45]. Table 14.2 displays some recent studies that have focused on removing several dissolved heavy metals and organic pollutants with the use of surface-modified walnut shell particles [46–50]. As noticed, all the tabulated works focused on producing active sorbents from the walnut shell particles after surface modification, through activation at high temperature or/and with the use of strong acid/bases or/and different agents. Also, the modified walnut shell particles were used to treat heavy metals, pharmaceuticals, and toxic organic molecules only in batch adsorption experiments, without continuous investigation inside fixed bed column that operates under various hydrodynamic conditions [46–50].

14.2.3 Weak Acid Cationic Exchange (WAC) Unit

In WAC, alkalization of water is carried out by using WAC resins (i.e., carboxylic type acids), in order to remove the divalent ions of Ca^{2+} and Mg^{2+} generated from WLS unit [17]. The WAC resins are spherical beads of a network of cross-linked polymers [34]. The cross-linked polymers are composed of functional groups with fixed co-ions that are negative charge located on each functional group along with the polymer matrix [34]. These co-ions are pre-saturated with cations that are mobile and free to move on the pores of the polymer matrix [34]. With adding these resins to the PW phase, the cations tend to diffuse in the bulk phase at high rate, yielding negatively charged resins [34]. Consequently, the counterions presented in the wastewater solution can migrate into the negatively charged resin phase and replace the cations stoichiometrically till attaining the equilibrium [34]. At equilibrium, the concentration differences of the ions are balanced that maintain the electroneutrality between the bulk solution and resin phase [34]. The WAC resins are generally described by formula of R-COOH that are able to remove the alkalinity from the carbonate hardness by the following equation [17]:

$$2\mathrm{RCOOH} + \mathrm{Ca}\left(\mathrm{HCO_3}\right)_2 \Rightarrow \left(\mathrm{RCOO}\right)_2 \mathrm{Ca} + 2\mathrm{CO_2} + 2\mathrm{H_2O} \tag{14.11}$$

$$2\mathrm{RCOOH} + \mathrm{Mg}\left(\mathrm{HCO_3}\right)_2 \Rightarrow \left(\mathrm{RCOO}\right)_2 \mathrm{Mg} + 2\mathrm{CO_2} + 2\mathrm{H_2O} \tag{14.12}$$

Also, the removal of divalent ions by WAC resin can be done as follows [17]:

$$2\mathrm{RCOOH} + \mathrm{M^{2+}} \Rightarrow \left(\mathrm{RCOO}\right)_2 \mathrm{Ca} + 2\mathrm{H^+} \tag{14.13}$$

$$\mathrm{H^+} + \mathrm{HCO_3^-} \Rightarrow \mathrm{H_2O} + \mathrm{CO_2} \tag{14.14}$$

$$2\mathrm{H^+} + \mathrm{CO_3^{2-}} \Rightarrow \mathrm{H_2O} + \mathrm{CO_2} \tag{14.15}$$

The carboxylate resins require alkaline species in the water to react with the more tightly bound hydrogen ions[17]. Thus, the resins are able to remove Ca, Mg, and heavy metals (i.e., Pb) from sulfates after conversion to sodium resins as shown below [17, 34]:

$$\mathrm{RCOOH} + \mathrm{NaOH} \Rightarrow \mathrm{RCOONa} + \mathrm{H_2O} \tag{14.16}$$

$$2\mathrm{RCOONa} + \mathrm{CaSO_4} \Rightarrow \left(\mathrm{RCOO}\right)_2 \mathrm{Ca} + \mathrm{Na_2SO_4} \tag{14.17}$$

$$2\mathrm{RCOONa} + \mathrm{MgSO_4} \Rightarrow \left(\mathrm{RCOO}\right)_2 \mathrm{Mg} + \mathrm{Na_2SO_4} \tag{14.18}$$

$$2\mathrm{RCOONa} + \mathrm{PbSO_4} \Rightarrow \left(\mathrm{RCOO}\right)_2 \mathrm{Pb} + \mathrm{Na_2SO_4} \tag{14.19}$$

Table 14.2 Most recent studies that have reported the using of surface modified walnut shell filter particles to treat several types of heavy metals, pharmaceuticals, and toxic organic molecules [46–50]

Number	Title	Methods	References
1	Removal of Cr(VI) from aqueous solutions by modified walnut shells	The nutshell particle surfaces were only treated by acids at high temperature (>200 °C).	[46]
		The modified nutshell particles were used to remove the chromium.	
2	Selective removal of cesium from aqueous solutions with nickel (II) hexacyanoferrate (III) functionalized agricultural residue–walnut shell	The nutshell surface modification was chemically done by $NiCl_2$ and the treatment of $K_3[Fe(CN)_6]\cdot 3H_2O$.	[47]
		The modified nutshell was used to remove cesium ion (Cs^+) from aqueous solutions.	
3	Adsorption of naphthalene from aqueous solution onto fatty acid modified walnut shells	The surface of the nutshell was modified by fatty acid.	
		The removal was tested for naphthalene.	
4	Highly synergistic effects on ammonium removal by the co-system of *Pseudomonas stutzeri* XL-2 and modified walnut shell biochar	The walnut shell particles were modified by pyrolysis at 300 C and impregnated by 1.0 M NaOH. Then the material was washed, dried at 60 °C, pyrolyzed at 450 °C, and impregnated by 0.5 M $MgCl_2$ for 4 h.	[48]
		The modified material was used as sorbent for ammonia.	
5	Adsorption of lead ion from aqueous solution by modified walnut shell: kinetics and thermodynamics	The walnut shell particles were treated by acid and maleic anhydride to be used as adsorbent for lead.	[49]
		The modified walnut shell particles were used to remove lead from water.	
6	Characterization of metal oxide-modified walnut-shell-activated carbon and its application for phosphine adsorption: equilibrium, regeneration, and mechanism studies	The walnut shell particles were first activated at elevated temperature. Then they were modified by metal oxide.	[50]
		The modified nutshell particles were used to remove phosphine (PH_3) from water.	

Considering the previous reaction sets, WAC resins exhibit marked degree of volume expansion after conversion from hydrogen to sodium form, which is considered as one of their major disadvantages [17, 34]. Their permeance is also sensitive to the medium's pH, such that the apparent capacity increases to the maximum at pH higher than 11 (above pK_a) [17, 34]. Applying organic resins in cationic exchanger significantly contributes in increasing the total dissolved solids, causing numerous operational problems like fouling of pipelines and equipment and clogging of injection wells [17, 34].

Hence, replacement of the current scheme with a process which can separate almost all silica and reject more than 90% of the dissolved organic matters will considerably reduce the capital and operating costs due to the reduction of size and number of steam generators. Accordingly, many authors have made considerable efforts to come up with emerging technologies in order to modify or replace the current treatment train with more effective and economical solutions [17, 34].

14.2.4 Emerging Techniques for SAGD Produced Water Treatment

In the last decade, many studies have reported some emerging techniques for treatment of SAGD produced water that depends on either chemical or membrane filtration processes (Table 14.3) [51–56]. As shown from Table 14.3, most of the recent studies focused on fabrication of effective and inherently fouling-resistant membranes with better performance than some commonly used membranes (i.e., ceramic membranes) that showed some serious challenges [52–56]. These challenges have led the researchers to develop various fouling remediation techniques to break up surface deposits, backflushing with permeate and the use of many different chemical cleaning agents [52–56] . These modified membranes showed great potential in treating SAGD produced water, under well-controlled temperatures and pH [52–56].

Basically, the surface of the commercial ceramic membranes is highly hydrophobic because of the charged hydroxyl groups that occupy the selective layer [52–56]. Thus, the predominant surface charge of a ceramic membrane is pH-dependent given the isoelectric point of the selective layer's constituent metal oxide [52–56]. In many cases, controlling the pH of the feed solution so that the membrane surface charge leads to the electrostatic repulsion of charged foulants is an adequate method of fouling alleviation [52–56]. However, bituminous foulants like asphaltenes possess amphoteric functional groups, meaning that they can exhibit both positive and negative surface charges at any given feed pH [52–56]. To mitigate the interaction between amphoteric bitumen and the hydroxyl groups, the membrane surface can be chemically modified by a highly hydrophilic polymer (i.e., charge-neutral polyethylene oxide (PEO) functional silanes) in a way that reduces its electrostatic charge. On the other hand, implementing single-layer cellulose-based membranes toward thin-film composite (TFC) polyamide (PA)-based membranes showed superior permeation properties with better flux and selectivity, compared with commercially available membranes of TFC [52–56].

Implementing these surface modifications for the membranes provided successful forming of hydrophilic layers on the membrane surface that subsequently improves membrane flux and mitigated any irreversible effects [52–56]. However, the application of these modified membranes requires well-tuned and strict environment (i.e., temperature and pH), such that high pH and temperatures resulted in better separation performance, which enlarge the operational costs. Additionally,

Table 14.3 Most recent emerging techniques that have been reported for treatment of SAGD produced water [51–56]

Number	Topic	Material and methods	Main results	References
1	Treatment of oil sands produced water using combined electrocoagulation and chemical coagulation technique	Hybrid electrocoagulation-chemical coagulation (EC-CC) process has been used as an alternative to conventional chemical processes for the treatment of steam-assisted gravity drainage (SAGD) produced water under influence of various electrode material, cell configuration, pH and temperature of the solution, chemical coagulant dosage, intensity of the electrical current, mixing rate, and treatment time.	Parameters except the electrode arrangement had a significant effect on the removal of silica and TOC.	[52]
			The chemical coagulant and the treatment time had the most significant contribution to the efficiency by 40% and 26%, respectively.	
			The optimum condition for the highest TOC removal efficiency (39.8%) was obtained by applying 0.34 A to Al electrode in a bipolar (BP) configuration when the pH, temperature, coagulant concentration, mixing rate, and reaction time were set to 8, 60 °C, 200 mg/L, 700 rpm, and 90 min, respectively.	
2	Developing high-throughput thin-film composite polyamide membranes for forward osmosis treatment of SAGD produced water	High-performance thin-film composite TFC membranes by an innovative adjustment of interfacial polymerization (IP) reaction between m-phenylenediamine (MPD) and trimesoyl chloride (TMC) at the surface of a polyethersulfone (PES) microporous support.	Reducing the temperature of the organic solution down to −20 °C effectively reduced the thickness of the PA selective layer and thus significantly enhanced water permeation through the membranes.	[53]
			The water flux increased more than double for membranes prepared at 25 °C to 38.5 and LMH at −20 °C, when 3 M NaCl solution and de-ionized water were used as draw and feed solutions, respectively.	
			The performance of lab-synthesized TFC membranes was also evaluated for the treatment of boiler feedwater (BFW) of steam-assisted gravity drainage (SAGD) process.	

Number	Topic	Material and methods	Main results	References
3	Silane surface-modified ceramic membranes for the treatment and recycling of SAGD produced water	Membranes were synthesized from ceramic modified by highly hydrophilic and neutral organosilane.	The modification was successful in mitigating the irreversible fouling caused by bituminous ultrafines.	[54]
			The permeate flux of the 150 and 300 kDa membranes more than doubled after modification in a 20% silane solution.	
			The filtered water obtained from the modified membranes was of superior quality to that of the untreated membrane, as evidenced by total organic carbon analysis.	
4	Surface-modified multi-lumen tubular membranes for SAGD produced water treatment	Membranes were made from multi-lumen tubular ceramic membranes chemically modified using several charge-neutral polyethylene oxide (PEO)-based organosilanes. Membranes with a pore size of 10 nm and selective layers of either γ-Al_2O_3 or TiO_2 were modified based on protocols previously used on small-scale ceramic membrane disks.	Modification of γ-Al_2O_3 membranes by a 30% solution of straight-chain PEO-silane increased permeate flux by factors as high as 2.9.	[55]
			Modification of TiO_2 membranes also improved permeate flux.	
			Flux recovery factors upon backflushing increased from 1.3 to 1.6.	
			The decline in performance when switching to a SAGD feed, with a higher pH, total organic carbon, and alkalinity, was significantly less severe for modified TiO_2 membranes compared to unmodified counterparts.	
			Surface modification of tubular ceramic membranes with PEO-based silanes was successful in improving the rejection of bituminous foulants from the membrane surface.	

(continued)

Table 14.3 (continued)

Number	Topic	Material and methods	Main results	References
5	Development of antifouling membranes using agro-industrial waste lignin for the treatment of Canada's oil sands produced water	Antifouling polyethersulfone (PES) membranes were prepared from industrial waste derivative of lignin, sulfonated Kraft lignin (SKL), containing highly hydrophilic and negatively charged functional groups, as a bulk modifier for the fabrication.	The modified membrane containing the highest amount of SKL additive (3 wt.%) exhibited profound enhancement in the flux recovery ratio from 52.2% to 98.2% compared to the pristine PES membrane against the complex mixture of organic pollutants in SAGD produced water.	[56]
			The rejection of the organics decreased only slightly from 61.7% for the pristine membrane to 56.1% for the 3 wt.% SKL-embedded membrane, while the permeability and molecular weight cutoff (MWCO) increased by 43.3 LMH/psi and 144 kDa, respectively.	
6	An integrated oxy-cracking, nano-adsorption, and steam gasification processes for treatment of SAGD produced water	In treatment of SAGD produced water samples, the oxy-cracking technique is used as a pre-treatment step in order to generate solubilized organic intermediates under basic conditions at temperatures (473–253 K) and at a pressure of 1000 psi. The oxy-cracked organics from SAGD effluents were adsorbed onto silica-embedded NiO extrudates inside a packed-bed column under various operational parameters (i.e., flow rate, inlet concentration, and bed height. The catalytic steam gasification reaction was performed on the adsorbed species to produce syngas from the adsorbed organic matters and to regenerate the extrudates in order to use them sustainably for further cycles.	The integrated method was successfully implemented to reduce the total organic carbon from SAGD produced water.	[57]
			The oxy-cracking reaction involved a deep oxidation process flowed by a partial oxidation reaction with formation of oxy-cracked intermediates solubilized in the liquid phase.	
			The results showed that the column was able to remove greater amounts of TOC molecules at low flow rates, low inlet concentrations, and high bed heights.	
			The extrudates were regenerated and reused for two cycles of adsorption via the catalytic steam gasification process.	

Number	Topic	Material and methods	Main results	References
7	TOC removal by nanoparticles embedded into the diatomite at industrial level field test rotary drum filter tests	Iron oxide nanoparticles were prepared by coprecipitation method and embedded into a 22.7 kg of diatomite at mass ratios of 0.5, 1, and 2 wt.%, by preparing them separately in a pre-coat slurry mix tank over a period of 65 min. The slurry mixture of embedded nanoparticles in diatomite was used to coat the rotary drum filter (RDF). The RDF applied vacuum that sucked the TOC molecules onto the drum pre-coated surface and the effluent wastewater was pumped out to the discharge tank. The effluent samples were periodically collected, and their TOC concentrations were measured as the time proceeding during the test. Each experiment was conducted at constant feed flow rate, amount of diatomite.	The results showed that the breakthrough time and TOC removal efficiency were increased by increasing the concentration of nanoparticles embedded onto the diatomite. Enhancing the employed amount of diatomite whether its embedded with nanoparticles or not significantly influenced enhanced the TOC removal efficiency.	[58]
8	Iron hydroxide nanoparticles anchored on the walnut shell filtration media for simultaneous removal of silica and TOC from SAGD produced water.	Simultaneous remediation of silica and TOC was achieved by modifying the surface of the walnut shell with anchoring low mass percentages (e.g., < 5wt%) of iron (hydroxide) nanoparticles under moderate hydrolysis conditions (e.g., temperature, hydrolysis time, and concentration of nanoparticle precursor). The nanoparticles anchored on walnut shell particles (WS-NPs) were fully characterized, and their effectiveness toward the removal of TOC and silica was examined using batch and column experiments. Regeneration and recyclability of the spent materials were successfully investigated following direct backwashing and blade stirring methods.	The WS-NPs due to the presence of the nanomaterials showed an outstanding ability to remove TOC and silica, such that the modified material performed well in removing up to 85% of silica and TOC compared with the non-modified nutshell filter particles that showed <5% removal efficiency in the batch sorption tests. The packed column with WS-NPs and similar to the industrial operation showed an improved breakthrough behavior, without having channeling or pressure drop limitations. Regeneration cycles of the spent column were successfully done following direct backwashing and blade stirring methods.	[51]

(continued)

the synthesis methodologies followed in fabrication or surface modifying these membranes are not simple and need too many steps, which had significant environmental and cost downsides [52–56]. On the other hand, using combined electrocoagulation and chemical coagulation technique (study number 1) resulted in great performance in removing of silica and TOC [52]. However, attaining successful removal of silica and TOC required changing the medium pH and temperature, which is not industrially recommended. The table also includes another integrated technique that has been lately done for effective removal of TOC from SAGD produced water samples through sequential oxy-cracking, nano-adsorption, and steam gasification processes, which schematically described in Fig. 14.2 [57]**.**

14.2.4.1 Nanoparticle as an Emerging Technique for Treatment of SAGD Produced Water

An Integrated Oxy-Cracking, Nano-Adsorption, and Steam Gasification Processes for Treatment of SAGD Produced Water

The oxy-cracking process (e.g., a combination of consecutive oxidation and cracking reactions) has been developed as a modification to the Zimpro process for sewage-sludge oxidation and as an alternative and efficient approach for converting residual feedstocks into value-added products [59, 60]. Ashtari et al. (2016) first employed the oxy-cracking process for converting n-C_7 asphaltenes into light hydrocarbons, thus making them more accessible to subsequent hydrocracking reactions [60]. Recently our research group has utilized the oxy-cracking process for converting residual feedstock like petroleum coke into various commodity products [61]. We also advanced the process selectivity and conversion by introducing the copper silicate catalysts[62]. The oxy-cracking reaction mechanism was inspired by the generalized lumped kinetics model for wet air oxidation, which assumes that not all the organic compounds present in wastewater are directly oxidized to CO_2 and H_2O, and instead, the rest of the hydrocarbons are converted to intermediate products which might be further oxidized [63]. However, during the oxy-cracking reaction, in an alkaline aqueous medium, regardless of the type of feedstock, it was stated that the reaction conversion was insignificantly influenced by oxygen pressure beyond 5.2 MPa [64]. Hence, working at this pressure range (3.4–5.2 MPa) and temperature (150–250°C) keeps the water under subcritical conditions. At subcritical conditions, the dielectric constant of water dramatically changes with the temperature, and thus the reaction media changes from ionic to radical reaction. For instance, the solid petroleum coke, under well-monitored oxidation and alkaline conditions, can be oxy-cracked to light organic compounds (i.e., carboxylic, naphthenic acids, and their corresponding organic compounds) [64]. In contrast to the oxidation reaction, the oxy-cracking reaction is able to convert the insoluble hydrocarbon to a more soluble form at moderate temperatures and pressure [64]. Enhancing the solubility of the organic species can reduce the selectivity of the oxidation reaction toward formation of carbon dioxide. Thus, involving the

oxy-cracking reaction into one process can create an eco-friendly and green technology. In treatment of SAGD produced water, as tabulated, the oxy-cracking technique has been employed for converting the existent inactive organic pollutants into active ones through oxygen incorporation with minimal emission of CO_2 [57, 65]. After that, the oxy-cracked organics from SAGD effluents were adsorbed onto silica-embedded NiO extrudates inside a packed-bed column that operated under various operational conditions (i.e., flow rate, inlet concentration, and bed height) [65]. Finally, the catalytic steam gasification reaction has been performed on the adsorbed species to produce syngas from the adsorbed oxy-cracked organic matter and to regenerate the extrudates to use them sustainably for further cycles of adsorption-gasification processes. The results have shown that this combined technique has been successfully implemented in reducing the high concentration levels of TOC from SAGD produced water samples to acceptable levels. In fact, the oxy-cracking reaction kinetics obeyed the lumped kinetic model involving two basic reactions [57]. The first reaction implied a deep oxidation process at which the organic species were completely oxidized to CO_2 and H_2O, while the second reaction involved a partial oxidation reaction with formation of oxy-cracked intermediates solubilized in the liquid phase [57]. Additionally, the in-house prepared SiO_2-NiO extrudates showed high adsorption affinity and TOC removal efficiency for the oxy-cracked hydrocarbons at low feed flow rate, low initial concentration, and high bed depth, then, great tendency for regeneration via gasification-adsorption processes. The photographs of the vials shown in Fig. 14 are for the virgin SAGD produced water (dark color), oxy-cracked SAGD produced water (yellowish color), and oxy-cracked SAGD produced water after adsorption in the packed-bed column (colorless). As seen by naked eye, a high degree of treatment was obtained for SAGD produced water, which can be indicated by converting their color from blackish to almost colorless. Thus, the treatment method performed well in removing the total organic carbon and silica from SAGD wastewater. This can be considered as a proof of concept for integrating oxy-cracking, adsorption, and catalytic steam gasification for cleaning up OSPW. Indeed, this approach is considered the first of its kind in the field of sustainable wastewater treatment. Even so, this combined technique was not fully efficient in removing silica and TOC simultaneously. Besides, applying this technique involved harsh conditions (i.e., high temperature, pressure, and pH), in order to optimize the solubility and selectivity of the oxy-cracked product, which could add extra operational costs and hamper the application at large scale. Indeed, weak monitoring of the oxy-cracking reaction allows to form undesirable by-products.

TOC Removal by Nanoparticles Embedded into the Diatomite at Industrial Level Field Test Rotary Drum Filter Tests

From Table 14.3, an industrial level field tests in a rotary drum filter (RDF) are included, which are commercially used to remove plenty of suspended and dissolved contaminants generated from different industrial effluents [58]. Figure 14.4

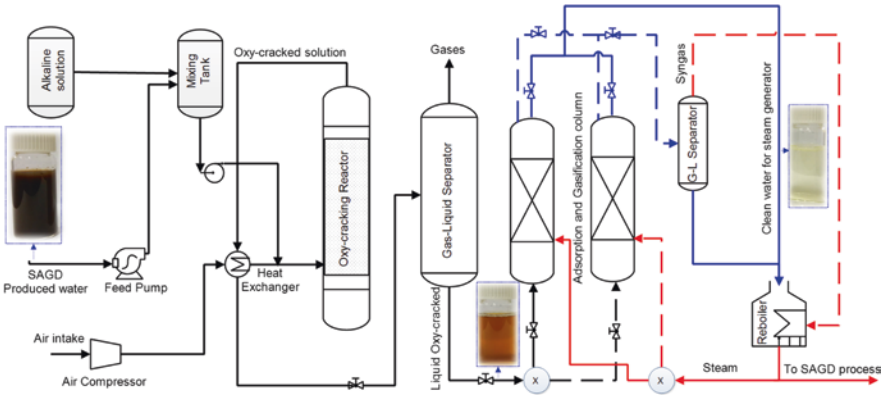

Fig. 14.3 A schematic representation of the proposed configurations for SAGD produced water using the oxy-cracking process. The vial images represent the SAGD wastewater before and after treatment by oxy-cracking at temperature 200 ºC and pressure 3.4 MPa and after 2 h adsorbed in the packed-bed column [66]. Permission related to the material excerpted were obtained from Elsevier, and further permission should be directed to Elsevier

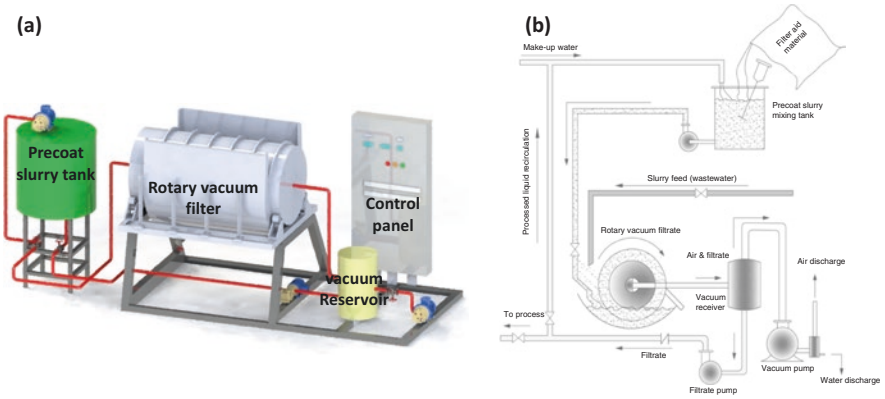

Fig. 14.4 (**a**) Three-dimensional and (**b**) two-dimensional schematic representations for a commercial rotary drum vacuum filtration unit (RDF) [58]. Copyright permission was obtained from the author

represents a schematic representation for the RDF, which mainly contains a drum rotating in a tub that accumulates the influent water. Before running the RDF, the drum is pre-coated with a filter aid material of diatomite [58]. The influent water is typically injected to the tub below the drum, which rotates through the influent water. Then a vacuum is applied that allows the wastewater to be sucked onto the drum's pre-coated surface, leading to the adherence of the suspended solid pollutants to the filter while it is rotating. The vacuum sucks the liquid portion through the filter media to the internal part of the drum, resulting in a filtrated liquid that is pumped away. Solids on the other hand adhere to the pre-coated surface. The drum then automatically passes a knife through the adhered solid and part of diatomite, revealing a fresh surface media. The RDF can work effectively in removing many

suspended pollutants. However, it has low efficiency in removing the dissolved TOC. Thus, the filter aid material was modified with anchoring low mass fraction (i.e., < 5 wt.%) of iron oxide nanoparticles, which were in-house prepared by coprecipitation method. As shown from the table, increasing the concentration of nanoparticles from 0.5 to 2 wt.% allowed to create capturing site that can effectively enhance the adsorption of the TOC molecules, which led to increasing the breakthrough time and TOC removal efficiency. Furthermore, it was also obtained that with increasing the feed flow rate, the breakpoint time and the adsorbed TOC molecules decreased [58]. The reason behind this is that when the flow rate increased, the residence time of TOC molecules was not enough for adsorption equilibrium to be reached at that flow rate, and the adsorption zone quickly saturates the precoated layer. Therefore, the contact time of TOC is very short at a high flow rate [58]. That subsequently reduced the TOC removal efficiency. On the other hand, when the feed flow rate is low, the TOC had more time to contact the sorption sites of adsorbent that led to achieving a higher removal of TOC molecules [67]. However, increasing the concentration of the nanoparticles embedded in the diatomite and the feed flow rate led to attaining channeling effect on the pre-coated filter aid layers. This channeling affect resulted from accumulation of more TOC molecules that tend to block the porous media and enhancing the pressure drop. Hence, it is highly recommended to operate under well-controlled operational parameters to avoid the pressure drop limitations that might occur due to embedding of nanoparticles.

Iron Hydroxide Nanoparticles Anchored on the Walnut Shell Filtration Media for Simultaneous Removal of Silica and TOC from SAGD Produced Water

As explained before, effectiveness of the walnut shell filter toward removal of many pollutants can be also enhanced via following some surface modification methods similar to those listed in Table 14.2. However, none of these studies have been continuously implemented via the column tests or to improve the depth filtration of the WSF unit toward removing of silica and TOC simultaneously [51]. In Table 14.3, study number 8 describes an innovative technique used to improve the removal of silica and TOC by anchoring low mass percentages of iron hydroxide nanoparticles on the walnut shell filtration. Presence of these nanoparticles enhanced the surface activity of the walnut shell filter particles, which create the potential to capture both silica and TOC [51]. The anchorage of iron hydroxide nanoparticles can be done chemically by two main steps: acid activation and formation of iron hydroxide nanoparticles under moderate hydrolysis conditions (e.g., temperature, hydrolysis time, and concentration of nanoparticle precursor). The purpose of the first step is permitting to generate open macropores and cavities that contribute in rendering diffusion sites that tend to accommodate the nanoparticles [51]. In the second step, iron hydroxide agglomerates in nanoscale are formed from thermal hydrolysis of ferric ions that originate from dissociation of ferric salt. Under aqueous conditions, the dissociative ferric ions are coordinately bonded with water molecules in the nature of aqueous complexes [68]. These complexes progressively go through

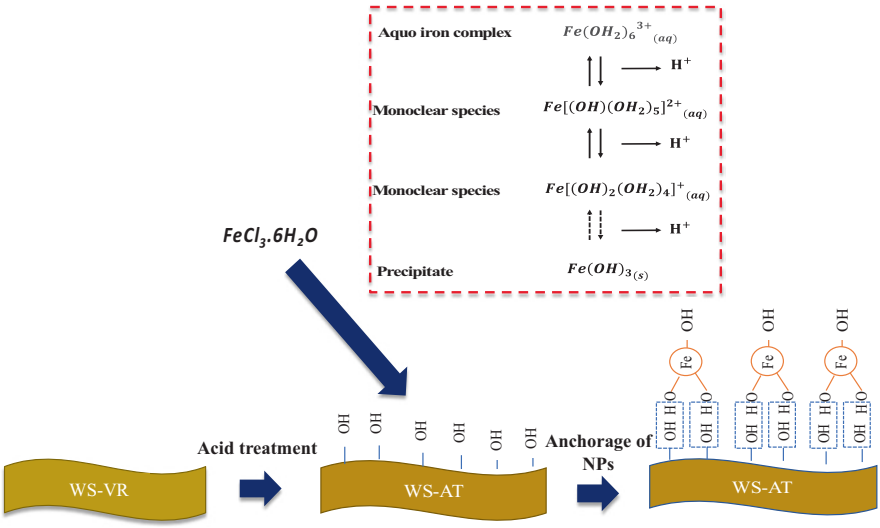

Fig. 14.5 Surface modification of the walnut shell surface (WS-VR) through acid treatment anchorage of iron hydroxide nanoparticles. Copy right permission was obtained from reference [51]

arrays of hydrolytic reactions as described in Fig. 14.5. During the hydrolytic reactions, deprotonation of the complexes is carried out yielding groups of soluble mono-clear and non-soluble species. Then, the generated species are able to be anchored on the hydroxylated filtration particles by:

1- Forming oxygenated bridges: The hydroxylated and acid treated particles interacted with one of the mono-clear species by forming oxygenated bridges through a nucleophilic substitution mechanism [69].
2- Bidentate adsorption: The hydroxylated species are adsorbed on the precipitate species of iron hydroxide by bidentate adsorption mechanism [68].

It can be concluded from the table that the filter aid particles due to the presence of iron hydroxide nanomaterials outperform in remediation of TOC and silica molecules in comparison with that achieved by applying the non-modified nutshell filter particles in the batch and column sorption tests [51]. The TFD calculations based on the theoretical adsorption energies have also proven that silica and TOC molecules adsorb more strongly to the surface of nanoparticle-functionalized walnut shell compared with the bare walnut shell [70–82]. Under continuous operations, the WS-NPs resulted in improved breakthrough behavior in the absence of any pressure drop limitations.

This clearly proves that applying the anchored walnut shell particles with nanoparticles can potentially form a high-quality water with low levels of both silica (<30mg/L) and TOC (<50mg/), meeting the strict requirements in the employed

boiler for steam generation. According to that, altering the non-modified walnut shell particles (WS-VR) with our modified once (WS-NPs) in the WSF should provide a replacement for the conventional treatment train, in which the conventional WLS, WSF, and WAC can be substituted with one single unit. Interestingly, to evaluate the regeneration option, three consecutive regeneration studies were successfully done on the spent column following direct backwashing and blade stirring methods. Evidence to date suggests that WS-NPs is a stable sorption/filtration medium, in that relatively small amount of iron hydroxide nanoparticles that have low tendency to be lost over time during treatment, regeneration, and backwashing steps. However, additional long-term testing is required to confirm these finding and to quantify the effective lifetime of the media.

14.3 Enhancing Settling and Dewatering of Mature Fine Tailings (MFT)

Various treatment processes, with varying levels of success and feasibility, have been used to speed up the settling rate of the fine particles in MFT and maximize the water recovery rate for reuse in the industry [83–86]. These treatment methods can be classified as natural, biological, physical/mechanical, and chemical techniques [25, 87]. With natural processes, the solid contents in the MFT are increased up to 45% by freeze-thaw technology, such that the tailings are allowed to be frozen during the wintertime and then thawed in the summer [25, 87]. At sub-zero temperatures, ice crystals are continuously growing to form segregated reticulated ice fine-grained structure, which converts the dispersed MFT slurry layers to more face-to-face compact layers [25, 87]. With thawing, the MFT compact layers tend to agglomerate into irregular four-sided polygons, causing a significant reduction in the moisture content. Additionally, some researchers have suggested the use of concentrated sulfuric acid before the freeze-thaw cycle for more reduction in the moisture contents [25, 87]. Implementing freeze-thaw technology, as a natural process, is labor intensive and time-consuming process [25, 87]. In biological process, on the other hand, active species are planted and grown up on a high-water content area by photosynthesis [83–86]. Afterward, the natural plants tend to consume the water by the respiration processes through the leaves and roots, which leads to dewatering of the tailings. However, creating the suitable environments for the plants is not possible all the time [83–86]. In fact, this method highly depends on the local climate conditions, and plants cannot grow in high saline and sodic environments. In the case of the physical/mechanical processes (i.e., filtration and centrifuge treatment), the most traditional one is filtration, which has low environmental impacts. Furthermore, centrifuging of the MFT requires a small storage area to generate tailings with 60% solid contents [83–86]. Filtration and centrifugation, however, are costly physical separation methods. Thus, the chemical treatment has remained as

the most adapted technology to enhance the flocculation and consolidation of MFT. Commercially, traditional consolidated tailings (CT) followed by paste tailing processes are consequently practiced to enhance the consolidation and water recovery rates of the MFTs [83–86].

14.3.1 Composite Tailing (CT) Treatment

In CT, massive quantities of coagulant aids such as gypsum, lime, acids, and acid-lime combinations are extensively introduced to generate unstable and non-segregating deposits with less water contents [88–90]. Both lime and gypsum are the mostly applied coagulant aids in CT due to their great tendency in forming residual calcium ions. These ions strongly eliminates the organic layer presented on surfaces of the stable MFT clay particles [88–90]. This subsequently enhances the aggregation of the clay particles in the form of non-segregating tailing slurry [88–90]. However, the recovered water due to the presence of high residual concentrations of calcium and sulfate might negatively impact the oil recovery process and the environment [88–90]. In fact, the presence of residual amounts of calcium ions has a deleterious effect on the bitumen recovery process and imparts hardness to water [88–90]. While rich water with high amount of sulfate ions often undergoes anaerobic reduction, releasing harmful gasses such as H_2S, which is highly toxic to the environment and living organisms [88–90]. Here in Alberta, some local companies developed the CT by injecting $Ca(OH)_2$ together with CO_2 into the freshly produced tailings, which precipitate the dissolved $Ca(OH)_2$ as $CaCO_3$, which can be removed by a further thickening process. Such modification allows to form crystals of $CaCO_3$ that tend to uptake the fine particles presented in the MFT as sediments.

14.3.2 Paste Tailing Processes

Paste tailing is defined as tailings that have been significantly dewatered using polymeric flocculants to a point where they do not have a critical flow velocity when pumped, do not segregate as they deposit, and produce minimal (if any) [88–90]. Thus, the paste tailing process relies heavily on the flocculation performance of the applied commercial flocculants, such as the polyacrylamide-based polymeric flocculants (PAM)-based polymeric flocculants, to enhance the water solid separation in the MFTs [84–86, 91–94]. In the presence of polymeric flocculants, the destabilized particles presented in the MFT are flocculated into two main stages, namely, perikinetic (microscale) and orthokinetic (macroscale) flocculation [34]. The perikinetic flocculation occurred after destabilizing the molecules on the wastewater solution randomly or immediately during their Brownian motion via thermal agitation. This stage of flocculation can produce flocs that have poor or strong settling

characteristics [34]. Orthokinetic flocs, on the other hand, generate developed particles that can be promoted by mechanical agitation. The mechanical agitation (by Jar test) induces a velocity gradient in the liquid, improving the contact between the particles. The previously mentioned stages have a significant value in optimizing the flocculation/consolidation period upon selecting the proper conditions [34].

Unfortunately, PAM-induced floccules are loosely packed and settled slowly, since they are not able to reasonably flocculate the fine tailing particles [84–86, 91–94]. More precisely, the backbone of PAM contains amide groups, which contribute in generating strongly bonded gel-like polymeric networks that retain large volumes of water, with poorly consolidating sediments [91–93]. To alleviate these issues, many studies focused their efforts on structurally modifying the PAM to dewater MFT more effectively than the commercial PAM. These structurally modified PAM can potentially destabilize the solid particles presented in the MFTs by several mechanism as explained in the next section.

14.3.3 Destabilization Mechanisms

Fundamentally, stability of the solid particles presented in the MFTs is governed by the intermolecular force between the clay particles, electrical double layer among the charged particles, which is observed by the DLVO theory [34].

In the MFT colloidal suspension, counterions in addition to negatively charged clay particles are presented. The clay particles due to their negative charges tend to have intrinsic electrical repulsion force, which is responsible for existing of steric stabilization [34]. In principle, major fraction from the counterions tends to migrate and electrostatically neutralize the negatively charged clay particles [34], while minor fractions from the counterions diffuse away from the clay surface. Hence, an equilibrium distribution is established from both competing actions, in which the concentration of the counterions is gradually reduced with increasing the distance from the clay surface. The ionic distribution of the diffused counterions is referred as Gouy layer [34]. According to Gouy definition, two layers (double layer) can be presented in the clay suspension. The first layer is made from the positively charged counterions next to the clay surface "diffusion zone," and the second layer is formed from the negatively charged clay surface itself. The thickness of the diffusion layer (κ^{-1}) in Å can be calculated in by using the following expression [34]:

$$\kappa^{-1} = 10^{10}\left[\frac{(2)(1000)e^2 N_A I}{\varepsilon\varepsilon_o kT}\right]^{-1/2} \tag{14.20}$$

where 10^{10} is the length conversion $\left(\frac{\text{Å}}{\text{m}}\right)$, 1000 volume conversion (L/m^3) , e is the electron charge ($1.6022\times10^{-19}C$), N_A Avogadro's number (6.022×10^{22} /mol), I is the ionic strength, $\frac{1}{2}\sum Z^2 M\left(\frac{mole}{L}\right)$, Z is the magnitude of positive or negative charge on the ion, M is the molar concentration of cationic or anionic species *(mole/L)*, ε is

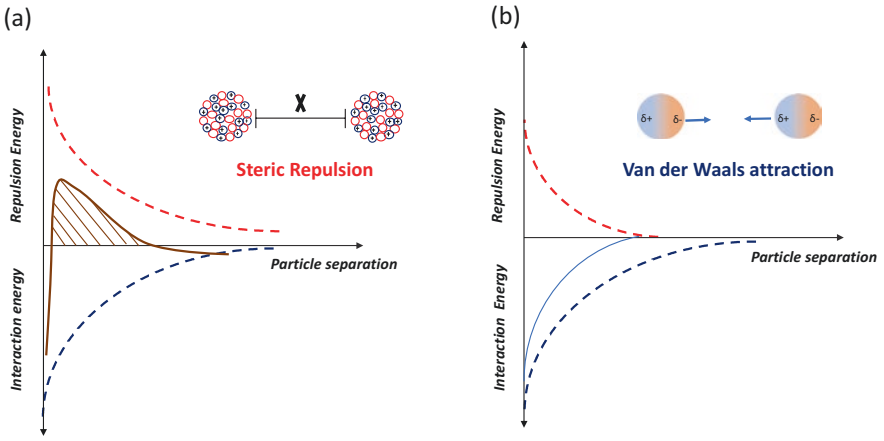

Fig. 14.6 Graphical representation of the stability mechanism according to DLVO theory with (**a**) and (**b**)without energy barrier. The graphical representation was drawn based on the concept available in reference [34]

the permissibility relative to vacuum ((*ε for water is* 78.54), ε_o is the permissibility in vacuum ($8.85\times\frac{10^{-12}C^2}{J.m}$), k is Boltzmann constant ($1.38\times10^{-23}J/K$), and T is the absolute temperature (K). Thickness of the formed double layer is strongly influenced by the physical properties of suspension, such as the temperature, bulk fluid concentration, and counterionic valence. For instance, at high ionic concentration and valance of counterions, counterions are diffused away from the Gouy's layer, resulting in double layer reduction [34]. However, Gouy's definition has limitations in accurately presenting the characteristic of the formed electrical double layer [34] . In fact, the ionic size and interaction between the clay surface, counterions, and medium are not accounted. Alternatively, Stern's theory came up with more practical model, such that it showed that the distance of the closest approach of a counterion to the charged surface is limited by the size of these ions [34]. Nevertheless, both Gouy's and Stern's theories cannot explain the stability of the solid particles presented in the tailings based on clay surface charged properties, interactions, and the balance between the repulsion and interaction forces in the suspension [34]. For better achieving of this, DLVO theory preciously describes the stability of the colloidal suspension by quantitatively consideration of (1) agglomeration and aggregation of the clay particles, (2) the force between charged particle interaction in the aqueous medium, and (3) the balance between the attractive van der Waals (vdW) force and the repulsive force caused by the overlap of electrical double layers surrounding the clay particles. In details, with using DLVO theory [65] (Derjaguin, Landua, Verwery, and Overbeek), the stability mechanism of the colloids can be quantitatively explained in terms of energy barrier. This energy barrier represents the difference between the repulsion and the attraction energy as presented in Fig. 14.6. The figure includes two possible cases with respect to the forces of repulsion. In the first case (Fig. 14.6a), the repulsion force is extended far in the

suspension, while in the second case (Fig. 14.6b), it was considerably decreased. In each figure, the net total energy is presented by the solid line [65].

For the first case, the net energy curve contains significant repulsion force that must be overcame when the particles are grouped together by van der Waals attraction, such that exceeding the energy barrier (the area under the solid line) by rupturing the net force that holds the particles far away from each other, which allows them to get attracted by van der Waals force [65]. In the second case, energy barrier exists to overcome, and the colloidal particles can be easily and rapidly flocculated by micro-flocculation. In the flocculation/consolidation process, the determination of the stability mechanism depends on the selected flocculant, its dosage, water/wastewater system solution, and mixing tools. Most importantly, the use of affordable and appropriate flocculant, depending on their action in destabilizing the colloidal particles, is consider the driving force for using flocculation/consolidation method in simultaneous removal of various polluting substances. Therefore, the use of vast categories of additives has been repeatedly reported, which fall into either hydrolyzing metal coagulants or polymeric flocculants [65].

Changing the ionic strength around the colloidal particles has significant effect on the stability mechanism. Double-layer compression, for instance, requires a reduction in the double layer around the colloidal particles, which causes changing on the ionic strength induced from addition of indifferent electrolyte, resulting in destabilizing of colloids under unstable conditions [65]. Consequently, colloids get close to each other with the presence of thin electric double layers. To more reduction of double layer, salts of counterion can be added, exceeding double layer repulsion that leads to coagulation of particles. However, this mechanism is industrially infeasible because it involves providing massive amounts of salts to achieve a practical destabilization of the particles [65]. Therefore, double-layer compression using salts was replaced by a destabilizing method of charge neutralization. Charge neutralization is often carried out by adsorbing the hydrolyzed metals or polymeric species on the clay surface [65].

Furthermore, high dosage of charge-neutralizing coagulants may lead to fast aggregation of the solids presenting on the colloidal suspension [65]. Interparticle bridging [65], other mechanism, can be achieved by chemical bonding or physical attachment of water-soluble polymer to the particle surface. In this mechanism, very small part of the polymer can adhere to the particle surface, while the bulk groups of the polymer chain cannot. These chains extend toward the solution, helping in adherence of the neighbor particles, forming bridged particles [65]. Then, the bridged particles during mixing are able to interact effectively with each other to form and develop flocs that are destabilized as a next step to induce aggregation and settling of large agglomerates. With the use of various cationic PAM-based copolymer, charge neutralization and interparticle bridging are considered as the most popular mechanisms responsible for enhancing the settling and dewatering of MFT. The aforementioned cationic PAM-based copolymers have been synthesized by bonding organic or inorganic agents to the PAM chain by grafting or copolymerization, in order to create organic-inorganic hydride flocculant, thermosensitive polymeric flocculants, and cationic copolymers with hydrophobic moieties [84–86, 91–94].

14.3.4 Flocculation Behavior with Inorganic-Organic PAM-Based Hybrid Copolymers

The enhancement of the flocculation efficiency of many polymeric flocculants was traditionally achieved by mixing them with inorganic microparticles [95–98]. However, controlling the dispersion of the microparticles in the presence of organic flocculants limited their applications [95–98]. To avoid such technical issue, many reviewers proposed combining inorganic agents (i.e., hydroxides of aluminum, calcium, magnesium, and iron) to the organic structure of PAM allowing to form inorganic-organic hydride copolymeric flocculants (Table 14.4) [95–98]. The studies listed in Table 14.4 show great potential of the organic-inorganic hybrid flocculants, in comparison with the commercial PAM, toward enhancing settling and consolidation of solid particles presented in MFT (study number 1) and kaolinite suspensions (studies number 2–4), via bridging and charge neutralization mechanisms [95]. Al-PAM, for instance, allowed to densify and destabilize the diluted MFT suspension through two stage processes: flocculation/sedimentation and filtration to reduce the dewatering time, indicating that the presence of positively charged $Al(OH)_3$ particles created strong affinity between aluminum and oxygen was responsible for Al-O linkage, which led to the adsorption of $Al(OH)_3$ on the silica surface [95]. Although applying both stages showed shortening in the filtration time of the diluted MFT sample (10–30 wt.% solid) from 25 min to 10, such process required high dosages of Al-PAM and generates a filtration cake with high moisture content (>23wt.%) [95]. The formed cake will require another separation process to recover the trapped moisture, adding extra cost for the process. The other studies reported the synthesis of other hybrid flocculants that depend on complex free-radical polymerization that is carried out under well-controlled temperature and drying conditions. The flocculation/consolidation performance of these inorganic-organic flocculants has been only investigated with kaolinite suspension not a real MFT. In fact, the optimal operating condition with the use of kaolinite suspension was reported between pH 2 and 2.5, which cannot be achieved with the real MFT suspension that has pH value around 9.

14.3.5 Flocculation Behavior with Stimuli-Responsive Polymers

In the last 10 years, using of stimuli-responsive polymeric flocculants to accelerate settling and consolidation rates has gained great attention by some authors. The stimuli-responsive polymers are defined as polymers that are able to change their conformation and solubility under certain conditions (i.e., temperature, pH, electromagnetic field, and ionic strength) [91, 99]. Among them, thermo-responsive polymers have been extensively utilized as flocculants for faster solid-liquid separation. Poly(N-isopropylacrylamide) (PolyNIPAm) has been reported as the most

Table 14.4 Most recent inorganic-organic hybrid flocculants used to enhance settling and dewatering of MFT and kaolinite suspension

Number	Title	Materials and methods	Main results	References
1	Al-PAM assisted filtration system for abatement of mature fine tailings	Al-PAM was synthesized in-house by polymerization of acrylamide monomer in an aluminum hydroxide colloidal suspension with $(NH_4)2S_2O_8/NaHSO_3$ as initiator at 40 °C. Al-PAMs of different molecular weights and aluminum contents were used. The Al-PAM of intrinsic viscosity of 750 cm/g, equivalent to an average molecular weight of two million Daltons, was identified to perform the best. In the current study, this selected Al-PAM was used exclusively to flocculate MFT after proper dilution from 30 wt.% to 10 wt.% solid.	Effective flocculation of ultrafine particles was confirmed by lower turbidity of supernatant after settling of diluted MFT with Al-PAM addition. When MFT diluted to 10 wt.% solids was filtered with 75 ppm Al-PAM addition, a filtration cake of 23 wt.% moisture content was produced after 25 min of filtration. To shorten the filtration time, a two-stage dewatering process was introduced: flocculation and thickening of diluted MFT, followed by filtration of sediments. With such an approach, filtration time could be further shortened considerably from 25 min to 10 min to produce a filter cake of 23 wt% moisture.	[80]
2	A novel flocculant of $Al(OH)_3$–polyacrylamide ionic hybrid	The hybrid $Al(OH)_3$–polyacrylamide (HAPAM) has been synthesized using a redox initiation system ($(NH_4)_2S_2O_8$–$NaHSO_3$) at 40 °C in aqueous medium. The flocculation behavior for 0.25 wt.% kaolin suspension was evaluated by spectrophotometry and phase contrast microscopy.	It was found that an ionic bond exists between $Al(OH)_3$ colloid and polyacrylamide (PAM) chains in the HAPAM and the flocculation efficiency of HAPAM is much better than that of commercial polyacrylamide (PAM) and PAM/$AlCl_3$ blend. The synergism between $Al(OH_{)3}$ and PAM in ionic HAPAM exists in the kaolin flocculating process. It can be attributed to electrostatic interaction between the positive $Al(OH)_3$ core and the negative particle of kaolin as well as the adsorption-bridging effect of polyacrylamide chains in the HAPAM.	[81]

(continued)

Table 14.4 (continued)

Number	Title	Materials and methods	Main results	References
3	Polyacrylamide-based inorganic hybrid flocculants with self-degradable property	Inorganic-organic hybrid flocculant was produced from inorganic soil-TiO_2-PAM hybrid materials by coating of titanium dioxide (TiO_2) nanoparticles on the surface of inorganic soils and subsequent polymerization of acrylamide (AM) on these nanoparticles under visible light. Inorganic soils including kaolin, bentonite, montmorillonite, and diatomaceous earth were used to control the volume and to reduce the cost, and the TiO_2 nanoparticles accelerated PAM degradation. To further investigate the flocculation performance of kaolinTiO_2-PAM hybrid materials, we prepared a 5 g/L kaolin suspension as the wastewater model with 1 ml, 2 ml and 4 ml of 5 g/L kaolin suspensions, respectively. Another 5 g/L kaolin suspension was used as the blank control. The solutions were stirred identically (i.e., in a "jar test" apparatus) at 150 rpm for 30 s and 60 rpm for 5 min, followed by 15 min of settling.	This hybrid material holds great promise in dewatering technologies and environmental protection for the reserves of oil sand. In the first 5 min, flocculation was obvious due to the adsorption and bridging effect of PAM, as evidenced by floccules at the bottom. With extended time, the transmittance increased gradually, indicating that the content gradually became clear. When 2 ml flocculant was added, the flocculating effect reached optimum. Excess flocculant affected the transmittance of the solution. Compared to traditional PAM-based hybrid flocculantskaolin-TiO_2-PAM hybrid material allowed "degradation by itself".	[82]
4	Flocculation of kaolin in water using novel calcium chloride-polyacrylamide ($CaCl_2$-PAM) hybrid polymer	A novel calcium chloride-polyacrylamide hybrid polymer has been synthesized by a redox initiation system by using $(NH_4)_2S_2O_8$ and $NaHSO_3$ to initiate free-radical solution polymerization of one molar acrylamide solution at 50 °C. One mole of calcium chloride was blended with polymerized acrylamide solution to synthesis a novel inorganic–organic composite polymer ($CaCl_2$-PAM hybrid polymer). Flocculation performance of kaolinite suspension was tested at various dosage and pH.	The kaolin suspension flocculation was found to be pH and dosage dependent. Response surface methodology was done using central composite design and showed that the $CaCl_2$-PAM hybrid polymer was able to reduce >98.0% of turbidity. The optimal operating condition was reported between pH 2 and 2.5 and dosage between 2 and 3 mg/L.	[83]

commonly applied thermosensitive polymeric flocculant [91, 99]. This polymer can be adsorbed on the surface of the clay particles by hydrogen bonding at temperature below the lower critical solution temperature (LCST) that is about 32 °C [91, 99]. With enhancing temperature above the LCST, significant phase transition can occur, at which the coil size is reduced by one third of the original size, leading to convert the polymer from hydrophilic to hydrophobic [91, 99]. The hydrophobic interaction is essentially controlled by the isopropyl groups that tend to be limited with formation of intra-chain interactions below the LCST [91, 99]. Thus, primary aggregation step is carried out by heating the wastewater thermosensitive polymer suspension above LCST, and once the big flocs are formed, the sediments are cooled down by secondary consolidation step, so the polymer becomes hydrophilic again and detaches from the particles; thus, the small particles can fill the gap between flocs to further enhance the consolidation [91, 99]. However, the thermosensitive polymer of PolyNIPAm is non-ionic and cannot neutralize the negatively charged clay particles, which limits its application in flocculation of fine clay particles. Thus, many researchers have done many attempts on introducing cationic groups with hydrophobic moiety to polyNIPAm in order to achieve higher flocculation ability [91, 99]. Table 14.5 displays some recent studies focused on applying diverse thermosensitive copolymers that are synthesized by copolymerization of N-isopropylacrylamide (NIPAm) with some hydrophobic moieties such as 2-aminoethyl methacrylamide hydrochloride (AEMA), 5-methacrylamido-1,2-benzoboroxole (MAAmBo), 2-aminoethyl methacrylamide hydrochloride, and poly(acrylamidest-diallyldimethylammonium chloride) (poly(AAm-st-DADMAC)), to create thermosensitive copolymers that are able to effectively flocculate and consolidate the fine solid in kaolinite suspension [91, 99]. As shown, significant enhancement in settling and dewatering has been achieved by flocculating the MFT and kaolinite suspensions with application of these thermosensitive copolymers in comparison with commercial anionic PAM. However, using thermosensitive polymers for large-scale application as flocculant for MFT has some downsides, related to the energy needed to heat up the slurry above the LCST and utilizing excess dosage of polymers to ensure good coverage of particle surfaces to induce aggregation above LCST [91, 99].

14.3.6 Flocculation Behavior with Hydrophobically Modified Polymeric Flocculants

Copolymerization of acrylamide (AC) with other hydrophobic monomers such as polypropylene oxide (PPO), hyperbranched functional polyethylene (HB*f*PE), and diallyl dimethylammonium (DADMAC) is one of the most commonly used approaches to enhance the dewaterability of the MFT aggregates (Table 14.6) [83, 92, 100]. In all the cases displayed in Table 14.6, the copolymer composition and average molecular weight were the most important factors affecting the settling and dewatering performance of MFT [83, 92, 100].

Table 14.5 Most recent studies that have used thermosensitive copolymers in enhancing settling and consolidation of kaolinite suspension and MFT [76, 84]

Number	Title	Materials and methods	Main results	References
1	Temperature- and pH-responsive benzoboroxole-based polymers for flocculation and enhanced dewatering of fine particle suspensions	Random copolymers based on N-isopropylacrylamide (NIPAAm) containing 2-aminoethyl methacrylamide hydrochloride (AEMA) and 5-methacrylamido-1,2-benzoboroxole (MAAmBo) were synthesized by conventional free-radical polymerization at70 °C in oil bath. The polymerization was carried out in the inert atmosphere for 24 h. The polymers were purified by dialysis against double distilled deionized water for 4 days. The fine kaolinite suspension flocculation performance was evaluated in solid–liquid separation at various pH and temperatures.	The strong interactions between benzoboroxole residues and kaolin hydroxyl groups were evaluated for the first time in the flocculation of fine particle suspensions. The lower critical solution temperatures (LCSTs) of PAMN decrease because of the hydrophobic nature of the benzoboroxole moieties, resulting in strong hydrophobic interaction at temperatures higher than the LCSTs. Temperature- and pH-responsive polymer, P(AEMA51-st-MAAmBo76-st-NIPAM381) (denoted as PAMN) shows the ability to induce fastest settling at a low dosage of 25 ppm and under the condition of pH 9 and 50 °C. The accelerated settling rate is considered to be due to the strong adhesion of benzoboroxole residues to the kaolin hydroxyl groups, the electrical double layer force, and the hydrophobic force. During condensation phase, increasing the pH of sediment to pH 11 could attain the most compact sediments.	[84]

2	Flocculation and dewatering of mature fine tailings using temperature-responsive cationic polymers	Temperature-responsive copolymer with cationic charge was prepared with N-isopropylacrylamide (NIPAm) and 2-aminoethyl methacrylamide hydrochloride (AEMA) by conventional free-radical polymerization. The flocculation performance of the copolymer, poly(AEMA-st-NIPAm), was compared to five different mixture ratios of polyNIPAm and cationic poly(acrylamidest-diallyldimethylammonium chloride) (poly(AAm-st-DADMAC)). The effects of polymer mixture ratios, polymer dosages, and temperature on solid–liquid separation as a function of initial settling rates (ISR), supernatant turbidity, sediment solid content, and water recovery were investigated.	Poly(NIPAm) can facilitate particle aggregation by bridging and hydrogen bonding under lower critical solution temperature (LCST), whereas at temperature above LCST, the adsorption of poly(NIPAm) chains on particles can be enhanced by hydrophobic interaction. A two-step (25 °C → 50 °C → 25 °C) consolidation can further enhance the sediment solid content by polyNIPAm. The neutral property of polyNIPAm resulted in high turbidity of supernatant, mixing with poly(AAm-stDADMAC) increases the clarity of supernatant by neutralization of fine particles. The copolymer poly(AEMA-st-NIPAm) functions as a polyelectrolyte to enhance the polymer adsorption onto particles via electrostatic interactions, thus further improving ISR and supernatant clarity.	[76]

Table 14.6 Most recent studied focused on synthesis of hydrophobically modified polymers and their applications in enhancing settling and dewatering of MFT [68, 77, 85]

Number	Title	Materials and methods	Main results	References
1	Using acrylamide/propylene oxide copolymers to dewater and densify mature fine tailings	Acrylamide (AC) was copolymerized by micellar polymerization with different amounts of polypropylene oxide macromonomers (PPO) to produce PAM-PPO graft copolymers with different hydrophobicities and molecular weights at 65 °C. Flocculation and dewatering performance was evaluated by determination of initial settling rate (ISR), turbidity, capillary suction time (CST), and solids content after centrifugation of mature fine tailings.	The PAM-PPO copolymers dewatered and densified MFT more efficiently than a reference commercial anionic PAM supposedly because the PPO hydrophobic groups reduced the amount of water trapped inside the polymer floccules. The PAM-PPO copolymers had molecular weights ten times smaller than the reference anionic PAM flocculant, which reduced their viscosities and shear sensitivities. As a result, it is easier to mix these copolymers with tailings under a wider window of operating conditions. The aged MFT (stored for approximately 10 months) were more easily dewatered, especially at high solids content (20 wt.%).	[77]
2	Flocculation of oil sands tailings by hyperbranched functionalized polyethylenes (HB*f*PE)	A series of hyperbranched functional polyethylene (HB*f*PE) flocculants with functional group contents ranging from 30 to 50 mol% were synthesized at 35 °C. The synthesized copolymers were used to flocculate oil sands mature fine tailings diluted to a concentration of 20 wt.%.	MFTs (diluted to a concentration of 20 wt.%) treated with the novel HB*f*PE had higher settling rates, lower capillary suction time (CST), and lower turbidity than when treated with a reference polyacrylamide (PAM). Within the HB*f*PE series, the settling performance improved when the functional group content in the copolymer increased. When combined with centrifugation, the HB*f*PE flocculants generated sediments with higher solid contents than PAM within a shorter centrifugation time.	[85]

Copolymerizing different average molecular weights of AC and PPO (poly(AAm)-g-PPO) significantly influenced the flocculation of the MFT [83, 92, 100]. At low solid content MFT (2 wt.% solids), the flocculation performance of poly(AAm)-g-PPO was not similar to the anionic polyacrylamide (A-PAM) as indicated from the obtained values of ISR and CST [83, 92, 100]. In fact, the used dosages for the copolymer were much lower than that for the commercial PAM (optimum performance achieved at about 2000 ppm for A-PAM versus 10 000 ppm for poly(AAm)-gPPO) [83, 92, 100]. The reason behind this referred to the large average molecular weight of the A-PAM (around 17 million Daltons) compared with that of poly(AAm)-gPPO). It has been also obtained that the addition of calcium prior to flocculation with A-poly(AAm) may help in reducing the PAM dosage, since it increased the degree of pre-aggregation of the suspended solids [83, 92, 100].

At high solid content MFT (20 wt.%), on the other hand, the authors observed that poly(AAm)-g-PPO gave much better dewatering than A-PAM at their respective optimum dosages, as indicated by about ten times difference in the CST values measured after flocculation [83, 92, 100]. The authors have claimed that the reason for this was due to the presence of more hydrophobic segments in the in poly(AAm)-g-PPO in comparison with A-PAM, not to the molecular weight difference [92]. To verify this, the author compared the flocculation performance of equal molecular weights of neutral PAM (N-PAM) and poly(AAm)-g-PPO, and the results have proven that the copolymer could still dewater MFT much better than the neutral poly(AAm) (CST of about 40 s versus CST of about 400 s) [92]. Likewise, flocculating low solid contents MFT (5 wt.% solid) with A-PAM led to much higher ISR compared to that of hyperbranched functional polyethylene (HBfPE) flocculants, but the HB*f*PE outperformed when it was flocculated with 20 wt.% solids [92]. These results were attributed to the extremely larger molecular weight of the A-PAM (100 times higher than HBfPE) [100]. The authors have hypothesized that the high molecular weight plays limited role in flocculation performance when the distance between the solid particles presented in the MFT are shorter at high solid content [100]. These results are not in agreement with that obtained by using poly(acrylamide-codiallyldimethylammonium chloride) poly(AAm-co-DADMAC). In fact, the average molecular weight does not play a considerable role (within the relatively wide range examined from 90 to 1450 kg mol−1[83], it is conceivable that it will become a factor for much lower molecular weights) in determining the performance of the copolymer based on the CST and SRF analyses [83]. The authors showed that the cationic copolymeric composition statistically influenced the settling and dewaterability performance, such that the flocculation and dewatering performance was better in the presence of more cationic segments, suggesting that charge neutralization is the dominant mechanism in dewatering MFT [83]. It has been also reported from the same study that addition of more AC to the system of AAm-co-DADMAC enhanced the rate polymerization. However, presence of more AC lowered the dewatering performance of the copolymer. Therefore, presence of low mass fraction of AC might save some polymer for dewatering MFTs but sacrifices kinetics of the polymerization reaction, and polymerizations at lower rates are, in general, economically less favorable than at higher rates.

According to that, the flocculation/consolidation performance is highly influenced by the molecular weight of the hydrophobically modified polymeric flocculant, such that better dewatering performance can be achieved by the polymeric flocculants grafted with more segments of hydrophobic agents (i.e., high molecular weight) for the MFT samples with high solid contents. However, in industrial applications when dealing with thick MFTs (i.e., 30 wt. % solids), there should be a desired range of polymer molecular weights.

14.3.7 Emerging Techniques for Treatment of Tailings

In addition to their high stability, MFTs might contain plenty of toxic and nonbiodegradable organic compounds that cannot be discharged to the environment such as naphthenic acids (NAs) [65, 101]. Thus, some emerging technologies have been recently proposed to remove the highly toxic NA compounds and enhance the settling and dewaterability of the MFTs. Nafie et al. (2017), for instance, have reported using β-Cyclodextrin-grafted nanopyroxene as eco-friendly platform for selective removal of NAs [101]. Nafie et al. (2018) also have suggested using oxy-cracking technique to destabilize the solid particles presented in the MFTs in order to enhance their flocculation consolidation behavior without applying any polymeric flocculants [65].

14.3.7.1 Oxy-Cracking Technique for Settling and Dewaterability of Oil Sands Mature Fine Tailings (MFT)

With employment of the oxy-cracking technique, the solid particles presented in the MFTs can be destabilized without adding polymeric flocculants by simultaneous oxidation and cracking reactions at which the residual bitumen presented on the MFT particles are cracked and solubilized in the liquid phase. This subsequently allowed for agglomeration and fast settling of the solid particles presented in the MFT, as schematically described in Fig. 14.7. The oxy-cracking procedure was experimentally done by placing well-mixed MFT sample inside one Parr reactor along with a strong basic material (i.e., KOH), which acts as a solubilizing agent [65]. The strong alkaline material is added to the mixture to ensure that the oxy-cracked products are completely solubilized in the aqueous phases and not converted to CO_2. After that, the Parr reactor was tightly closed, allowing to the oxy-cracking reaction to carry out under the flow of oxygen at temperature range of 423–498 K and pressure of 1000 psi over time ranging from 0.25 to 2h [65]. After completion of the reaction, the reactor is opened to release the excess of oxygen and undesirable product (i.e., CO_2) [65]. Then, the oxy-cracked product was directly transferred to a graduated cylinder to record the initial settling rates (ISRs) and

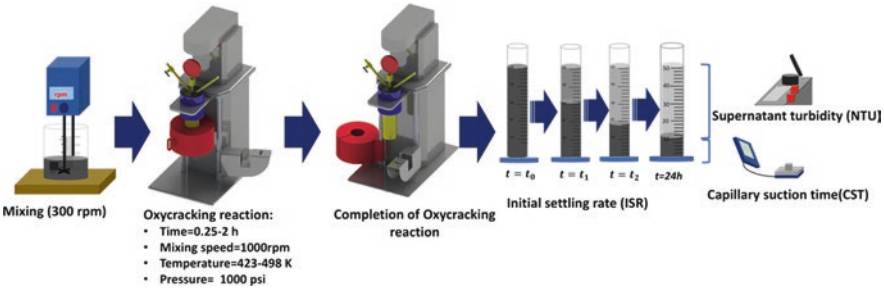

Fig. 14.7 Schematic representation for oxy-cracking of the diluted sample of MFT and testing its initial settling rate (ISR), supernatant turbidity, and capillary suction time (CST)

capillary suction times (CSTs) at different time interval [65]. The mechanism at which the oxy-cracking reaction was carried out for of the stable particle existed in MFT can be described by using a complex model [65]. In such model, the hydrocarbon species presented on MFT fine particles were initially decomposed in the presence of the free ·OH radicals into a variety of oxygenated intermediates, which tend to be cracked into different group of organic compounds, such as carboxylic and phenolic acids. Some of those intermediates were further oxidized to form carbonate or emitted as CO_2 in the gas phase [65]. Thus, the oxy-cracking reaction is able to break down these hydrocarbons and increase their solubility in the water phase, and thereby they detach from the fine solids. The fine solids will then agglomerate and settle faster [65]. The results showed that the mudline was diminished by 65% over 24 h for all the MFT samples after oxy-cracking in comparison with the non-oxy-cracked MFT. On the other hand, the consolidation (CSTs) tests arose fast and easy dewatering for the oxy-cracked MFT samples [65]. Furthermore, it has been obtained that both the temperature and residence time had no significant effect on settling rate. According to the CST measurements, it was also found that oxy-cracked MFT sample at 423 K, compared with the other samples, was easier to dewatered [65]. Although the oxy-cracking technique is an effective process for enhanced particle settling in oil sands tailings, it is not practical for massive quantity of MFT and non-economically feasible. In fact, oxy-cracking of great quantity of MFT requires larger size Parr reactor or running the reaction for longer time, which elevates the capital and operational costs. In addition, weak monitoring of the oxy-cracking reaction might cause releasing of extra amount of CO_2 that is harmful to the environment.

14.3.7.2 Using β-Cyclodextrin-Grafted Nanopyroxene for Naphthenic Acids (NAs) Removal

In the removal of NAs, β-cyclodextrin-grafted nanopyroxene has been used, combining the multifunctionality of B-cyclodextrins (BDN) and superficial ion exchange property of the nanopyroxene [102]. β-Cyclodextrin consists of hydrocarbon chains branched with large numbers of primary and secondary hydroxyl groups, creating lipophilic cavities [102]. Due to their biocompatibility and high affinity toward adsorbing several macromolecules, β-cyclodextrin has been commonly used to for wastewater treatment fields [102]. Thus, successful grafting of β-cyclodextrin on the surface of nanopyroxene allowed to create a novel adsorbent with excellent characteristics, which have a strong ability to capture complex organic pollutants, such as NAs. However, the nanopyroxene, without primarily functionalizing it with a dual affinity agent, cannot be grafted by the β-cyclodextrin [101, 103]. Thus, the nanoparticle surface was firstly coated with an organic-inorganic hybrid bridge of 3-glycidyloxypropyl trimethoxysilane (TG3), as shown in Fig. 14.8. In fact, the TG3, in the presence of toluene, is covalently bonded to the surface of the nanopyroxene by creating methoxy oxygenated sites [101, 103]. As a second step, the hydroxyls on the surface of BDN are activated by dissolving the dried monomer in an organic solvent of N,N-dimethylformamide (DMF) in the presence of a basic catalyst of sodium hydride, and then the mixture is dried, and its slurry product is added to a reflux system [102]. The slurry product in addition to the previously prepared solution of nanoparticles is mixed together for two hours at high temperature (i.e., 423 K). Such conditions allow for opening the epoxy ring for the

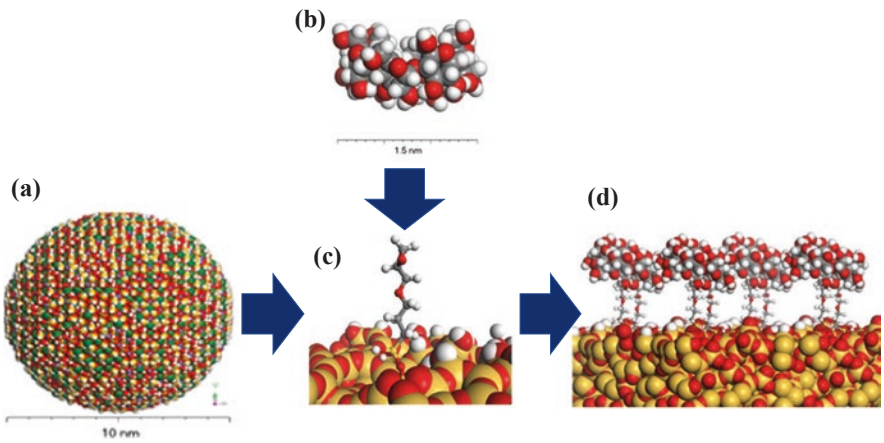

Fig. 14.8 CPK representation for the (**a**)10 nm of nanopyroxene (PNPs), (**b**) side view of β-cyclodextrin (BCN) molecule, (**c**) 45 ° perspective view presenting the primary coating PNPs with 3-glycidyloxypropyl tri-methoxy-silane (TG3), and (**d**) side view for the grafted nanoparticles of PNPs with BCN (PNPs-BCN) interacted with two hydrolyzed TG3 molecules. Red atoms represent oxygen, gray atoms represent carbon, white atoms represent hydrogen, and yellow atoms represent silicon [101]. Permissions related to the material excerpted were obtained from the American Chemical Society (ACS) and further permission should be directed to ACS

interaction by nucleophilic substitution with the activated O^- from the hydroxyls presented on the monomer [102]. The cavities presented on the structure BDN allows the accommodation of large and complex organic molecules such as naphthenic acids via adsorption [101]. These cavities are generated due to the distribution of the oriented units of the glucose molecules that is in the form of circular cones on the structure of BDN [101]. These trapping cones on the BDN are composed of seven methyl alcohol groups that are held together in a unique structure by intermolecular forces other than those of full covenant bonds (host-guest interaction) [102]. The results have shown successful adsorption of NAs on the grafted nanoparticles after performing batch adsorption test for synthetic wastewater containing NAs. Nevertheless, these types of grafted nanoparticles are not easy to prepare and required following complex procedure which depends on sever conditions.

14.4 Oil Spill Removal

The oil spills, without an effective removal method, showed adverse impacts to ecosystems and the long-term effects of environmental pollution that calls for an urgent need to develop a wide range of materials for cleaning up oil from oil-impacted areas [104, 105]. Additionally, the oil spills generate oil-water emulsions with produced water, hampering their treatment and disposal processes through physical separation, chemical processes, or biological degradation [104, 106]. Thus, a wide range of materials for oil spill removal has been successfully implemented including dispersants, absorbents, solidifiers, booms, and skimmers [105–108]. Recently, many scientists argue that applying most of these materials for oil remediation can be toxic—some at least as toxic as dishwashing liquid—and could be more harmful to the environment than the oil itself [104]. Also, there is potential for dispersants to bioaccumulate in seafood. Alternatively, many less harmful porous absorbents with some attractive characteristics (i.e., hydrophobicity or oleophilicity and high uptake capacity) have been used due to their high performance toward removal of the oil spill at high capacity and the possibility of recovery from the oil spill site [108]. Adding these porous sorbents facilitates a change from liquid to semisolid phase, and once this change is achieved, the removal of the oil, by removal of the absorbent structure, then becomes much easier. Also, many porous materials can, in some cases, be regenerated [109]. However, these materials have limited recyclability, due to the need for an effective oil/water separation process after each sorption step. The sorbed oil also requires mechanical handling, filtration, or high-rate centrifugation procedures that cannot be obtained under continuous operations. Traditionally, the oil/water separation occurred following standards like ASTM F716 and ASTM F726 [110]. These standards have shown inaccurate gravimetric measurements for the removed oil. Accordingly, applying these standards is inappropriate in describing the phenomena responsible for oil spill removal [111]. Recently, nanoparticle technology appeared to provide a practical and interesting alternative. As sorbents, nanoparticles have some unique properties, such as large

specific surface area per unit volume, high and fast equilibrium uptake, and great dispersibility for in situ treatment [112]. These properties have attracted many researchers to study their potential in the removal of oil spills via magnetite nanoparticles. Magnetite nanoparticles are economically favorable and easy to use as adsorbents in large-scale application. Also, they allow easy separation and recovery by applying an external magnetic field [8]. For the purpose of magnetic separation, magnetic nanoparticles can be synthesized into two forms: direct sorbent or in form of nanocomposite feature. Direct sorbent is formed when the magnetic nanomaterial occupies the whole structure of every single part of the nanoparticle [113]. Nanocomposite structure, on the other hand, is obtained when the magnetite is presented in nanoscale within the structure of the material to provide the desired function for the nanoparticles [103, 109].

14.4.1 Modified ASTM Protocol for Oil Removal Quantification

Under well-controlled conditions, the modified protocol for ASTM standard for oil spill absorption performance can be employed as shown in Fig. 4.9. The protocol allows for gravimetric evaluation of oil spills, which interact with the magnetic nanoparticles, without the employment of filtration or any other physical separation. Before testing the oil removal performance, a noncontact experiment should be initially performed to eliminate the real effect of the particle dispersion and their response toward the magnetic separation. During the experiment, a pre-weighted oil spill is simulated into a 500-mL beaker filled with deionized water at room temperature (Fig. 14.9a). After that, a certain amount of magnetic nanomaterial is added and distributed evenly on the oil under magnetic stirring for 2 min. Then, magnetic separation is used to withdraw the oil spill by placing a magnet 2 mm away from the water surface. Oil spill uptake is estimated by calculating the difference between the weight of simulated and magnetically separated oil spills (Fig. 14.9b-d). If there was a significant effect on self-magnetism of the particles, it should be subtracted from the uptaken oil spill.

14.4.2 Magnetic Oil Sorbent-based Nanoparticles

Due to the lack of stability, the naked iron oxide nanoparticles are either easily oxidized in air or tend to aggregate under aqueous conditions, which limits their application in remediation of oil spills. Thus, protection or functionalization procedures during or after the synthesis have recently been performed to apply the iron oxide nanoparticles more wisely [114–120]. These methods include coating or functionalization with organic or inorganic chemical agents, embedding the iron oxide

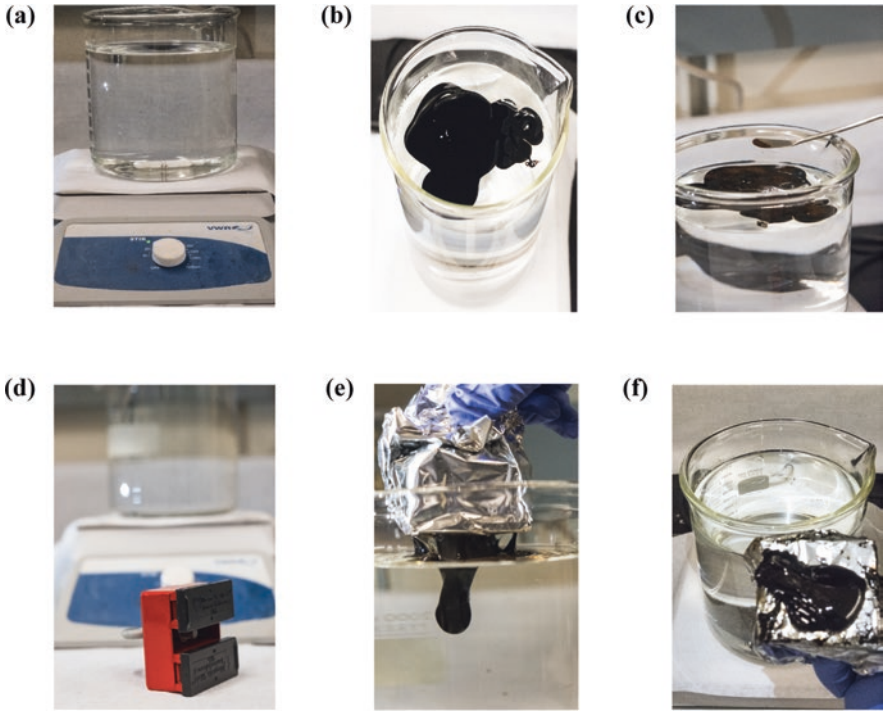

Fig. 14.9 Oil sorption test using a magnet, modification to ASTM F726-12. Photographs taken by the first author of this chapter

nanoparticles in polymer composites, and combining the iron oxide nanoparticles with activated carbon by physical and chemical methods [114–120]. Table 14.7 illustrates the most recent magnetic sorbents used for oil removal in addition to their functional materials, synthesis method, application, and their maximum oil uptake [114–120]. The table presents many magnetic oil sorbents that have been synthesized by combining the magnetic sorbents with organic compounds, macromolecules, biomolecules, polymers, inorganic materials, and activated carbon. These magnetic oil sorbents are characterized by having some favorable properties, including high sorption uptake, high hydrophobicity, high unsinkable properties to contact with oil (low density are easier to collect after sorption), ferromagnetism, and reusability [114–120]. The table shows that the magnetic structure of these magnetic sorbents mainly consists of iron oxide, which can be directly added in forms of powder or synthesized by several methods [114–120]. As shown from the table, the iron oxide has been directly added to the hydrothermally treated melamine di-borate (M_2B) to obtain magnetic hexagonal boron nitride [119]. On the other hand, the iron oxide can be synthesized by co-precipitation method, thermal decomposition, hydrothermal synthesis, and microemulsion. In co-precipitation, a chemical reaction is carried out between Fe^{3+} and Fe^{2+} salts in a highly basic solution and the absence of oxygen [68, 114–120]. For surface functionalization or coating, the

Table 14.7 Recently reported magnetic sorbents used for synthetic and real oil spill removal along with their synthesis methods, application, and maximum uptakes [99–105]

Number	Magnetic sorbents	Synthesis method	Application	Maximum oil removal	References
1	Magnetite functionalized with oleic acid	• The surfactant of oleic acid was used to modify ferrite nanoparticles by chemical precipitation • The -COOH groups of oleic acid have a high affinity with the Fe atoms of iron oxide	Crude oil	95 wt.%	[99]
2	Quaternized chitosan-coated magnetite	• Chitosan-coated iron oxide nanoparticles produced by grafting chitosan onto Fe_3O_4 coated with silica and 3-aminopropyltriethoxysilane (APTES)	Diesel-in-water emulsion	90 wt.%	[100]
4	Functionalized styrene (St) and sodium dodecyl sulfonate (SDS) with magnetite	• Synthesis was done by a two-step procedure • Magnetic Fe_3O_4 was prepared, and then, the silanization of Fe_3O_4 was performed by adding sodium dodecyl benzene sulfonate (SDBS) or sodium dodecyl sulfonate (SDS) followed by grafting of styrene	Diesel oil/lubricating oil	3g/g	[101]
5	Magnetic carbon nanotube sponges	• Fabrication was done by using ferrocene and dichlorobenzene as precursors by chemical vapor deposition	Diesel oil and gasoline	56 g/g	[102]

7	Magnetic coconut/palm shell-based carbon	• The sorbent prepared by pyrolyzing coconut shells. Then, activated carbon/Fe_3O_4 composites were obtained by in situ coprecipitation • An ammonia solution was added to the solution containing Fe^{3+}, Fe^{2+}, and activated carbon, and the mixture was heated to facilitate the binding of iron oxide nanoparticles to surface functionalities of the activated carbon	Premium oil	9.33 g/g	[103]
6	Hexagonal Magnetic boron nitride	• Magnetic boron nitride (MBN) by adding a stoichiometric ratio of 2:1 boric acid/melamine, melamine diborate (M_2B) precursor of boron nitride together with and powdered steel filings in proportion of 5% by mass. Precipitation of M_2B on the surface of the suspended steel filing particles. It is suggested that the use of a smaller volume of water and abrupt quenching are responsible for accelerating the precipitation of the precursor of boron nitride and facilitating the gathering of the iron particles from the steel filing within the M_2B.	Crude oil	53 g/g	[104]
7	Yeast-based magnetic bio-nanocomposite	Yeast-based magnetic bio-nanocomposite (Y-MG) can be prepared by mixing the yeast biomass with a heated suspension of magnetite nanoparticles that can be formed by the classical co-precipitation method under acidic conditions.	Of motor oil (NMO), mixed used motor oil (MUMO) and petroleum 28 °API (P28API)	3.5 gNmO/g, 0.2 gMUMO/g, and 2.8gP28API/g	[105]

coprecipitation method has been developed by adding functional materials or surface-active agents in the reaction media to reduce the aggregation and oxidation of naked iron oxide nanoparticles [114–120]. It has been reported that the size, shape, structure, and magnetic properties of iron oxide nanoparticles could be affected by the conditions of preparation, such as the type of Fe^{3+} or Fe^{2+} salt, the Fe^{3+}/Fe^{2+} ratio, the pH value, the reaction temperature, and the ionic strength of the media [121]. One disadvantage of the method is that during both the synthesis and purification process, the pH value has to remain high, which adversely affects the formation of uniform and monodispersed nanoparticles. Instead, high-quality monodispersed magnetic iron oxide nanoparticles can be formed by thermal decomposition method. In such method, the raw materials used frequently are organometallic compounds primarily including $Fe(cup)_3$ (cup = N-nitrosophenylhydroxylamine), $Fe(acac)_3$ (acac = acetylacetonate), or $Fe(CO)_5$ in an organic solution phase containing stabilizing surfactants under relatively high temperatures (200–300 °C) [68]. Unfortunately, the iron oxide generated by this method have a narrow size distribution and are highly monodispersed while only dissolvable in nonpolar solvents. With hydrothermal method, on the other hand, a chemical reaction occurred in aqueous solution containing iron salts under hydrothermal conditions, namely, a high-temperature aqueous solution (130–250 °C) and high vapor pressure (0.3–4 MPa) [68]. Through a hydrothermal process, the iron-based precursors could influence the size and shape of the magnetic products, and an appropriate hydrothermal temperature could cause an increase in the saturation magnetization.

Microemulsion, other synthesis process, is a thermodynamically stable method that generate magnetic sorbents from two immiscible phases in form water-in-oil micro-emulsion in the presence of surfactant [68]. The generated microemulsion consists of aqueous droplets stabilized by surfactant molecules in continuous phase [68]. The droplets, then, exist as reaction media to monitor the shape and size distribution of particles prepared by precipitating iron salts. Compared with the previously mentioned methods, many authors have proven that the formed nanoparticles by microemulsion method had a smaller size and higher saturation magnetization [68]. However, it is not simple and requires extra efforts for separating the nanoparticles and controlling their synthesis conditions. As shown in the table, the tabulated magnetic sorbents showed great potential in removing different types of synthetic and crude oils, especially the magnetic carbon nanotubes (study number 5), that outperformed with maximum uptake of 56g gasoline/g [118]. Nevertheless, these magnetic carbon nanotubes showed high bio-persistence. Hence, short- or long-term exposure of them might lead to harmful effect to the living organisms and human being (i.e., induced sustained inflammation, lung cancer, and gene damage in the lung). From the studies listed in the table, it is also worth to note that none from the first five studies have clearly described the mechanism at which the oil has been removed with the use of magnetic sorbents [114–120]. In most of the cases, it is not clear whether the removal of oil was due to surface effect (adsorption) or capillary effect (pore filling) of crude oil molecules on a hydrophobic magnetic sorbent, especially after surface modification [119]. Accordingly, sorption as general term is used to encompassing both “adsorption” and “absorption” phenomena,

such that both phenomena normally have been used interchangeably [119]. The last two studies, in contrary, had better observation for the mechanism involved in removing of oil by testing the magnetic sorbent in the removal of other dyes with opposite charges as model molecules, such that methylene blue (MB) and amaranth acid red (AR) [119]. By attaining the adsorptive removal isotherms from both model molecules, the involved mechanism in removal of the crude oil has been identified [119].

14.5 Conclusion

This book chapter examined the sources, characteristics, and water quality constrains for oil sands process affect water (OSPW) generated during the extraction or transportation of the bitumen and the different methods available for their treatment and disposal. Accordingly, this chapter comprehensively discusses the conventional physical/chemical treatment methods for the OSPW generated during oil extraction processes such as steam-assisted gravity drainage (SAGD) and surface mining. The chapter also provided an overview about the materials and methods that are traditionally utilized to remove the oil spills produced during oil transportation. In treatment of SAGD produced water, we critically reviewed the primary, secondary, tertiary, and emerging treatment technologies used to reduce the high concentration levels of silica, total organic carbon, and total hardness. We deeply reviewed some classical technologies implemented to enhance settling and consolidation of oil sand tailings, such as freeze-thawing, centrifugation, consolidated tailings (CT), and paste technologies (i.e., polymeric flocculation). Furthermore, we highlighted the advantaged and challenges of some recent magnetic sorbents used for oil spill remediation. As a result, we conclude that:

1- In the chemical treatment of SAGD produced water, introducing lime, ash, and slaked and non-slaked magnesium might enhance the concentration of divalent ions (i.e., Ca^{+2} and Mg^{+2}), which increases the need for another unit to be eliminated (i.e., WAC). This unfortunately adds additional disadvantages and extra operational and capital costs for the whole chemical treatment process. In the walnut shell filter unit, surface modification can be done for the filter aid material to enhance the removal efficiency of silica and TOC.
2- For enhancing settling and consolidation of fine tailings, the conventional technologies such as filtration and centrifugation are costly material or/and energy intensive physical separation methods. Thus, the chemical treatment has remained as the most adapted technology to enhance the flocculation and consolidation of MFT. Nevertheless, the chemical treatment requires adding of massive amount of coagulant aid (i.e., gypsum) and high molecular weight of polymeric flocculants (i.e., polyacrylamide-based copolymers).
3- Traditional remediation methods for the oil spills are either energy or material intensive. Additionally, many international scientists argue that most of the

applied materials for oil remediation can be toxic and could be more harmful to the environment than the oil itself. Many researchers have alternatively used magnetic sorbents that showed better performance and less environmental impact.

4- A family of eco-friendly nanoparticles, as part of emerging techniques, developed by Nassar's group at the University of Calgary has been effectively combined or integrated with the many physical and /or chemical processes utilized for remediation of OSPW.

References

1. S. Mekhilef, R. Saidur, A. Safari, A review on solar energy use in industries. Renew. Sust. Energ. Rev. **15**, 1777–1790 (2011). https://doi.org/10.1016/j.rser.2010.12.018
2. M. Bhattacharya, S.R. Paramati, I. Ozturk, S. Bhattacharya, The effect of renewable energy consumption on economic growth: evidence from top 38 countries. Appl. Energy **162**, 733–741 (2016). https://doi.org/10.1016/j.apenergy.2015.10.104
3. E.W. Allen, Process water treatment in Canada's oil sands industry: I. Target pollutants and treatment objectives. J. Environ. Eng. Sci. **7**, 123–138 (2008). https://doi.org/10.1139/S07-038
4. R.D. Schlosberg, R. Jordan, A more sustainable way to win oil from oil sands-part II. Characterization. J. Sustain. Energy Eng **5**, 13–28 (2017) https://www.energytoday.net/conventional-energy/sustainable-way-win-oil-oil-sands/
5. L. Pérez-Lombard, J. Ortiz, C. Pout, A review on buildings energy consumption information. Energy Build. **40**, 394–398 (2008). https://doi.org/10.1016/j.enbuild.2007.03.007
6. R.A. Frank, J.W. Roy, G. Bickerton, S.J. Rowland, J.V. Headley, A.G. Scarlett, C.E. West, K.M. Peru, J.L. Parrott, F.M. Conly, L.M. Hewitt, Profiling oil sands mixtures from industrial developments and natural groundwaters for source identification. Environ. Sci. Technol. **48**, 2660–2670 (2014). https://doi.org/10.1021/es500131k
7. S. Sorrell, J. Speirs, R. Bentley, A. Brandt, R. Miller, Global oil depletion: a review of the evidence. Energy Policy **38**, 5290–5295 (2010). https://doi.org/10.1016/j.enpol.2010.04.046
8. W. Pu, B. Wei, F. Jin, Y. Li, H. Jia, P. Liu, Z. Tang, Experimental investigation of CO2huff-n-puff process for enhancing oil recovery in tight reservoirs. Chem. Eng. Res. Des. **111**, 269–276 (2016). https://doi.org/10.1016/j.cherd.2016.05.012
9. G. Giacchetta, M. Leporini, B. Marchetti, Economic and environmental analysis of a Steam Assisted Gravity Drainage (SAGD) facility for oil recovery from Canadian oil sands. Appl. Energy **142**, 1–9 (2015). https://doi.org/10.1016/j.apenergy.2014.12.057
10. S. Canada, Oil Sands. Tailings Mine Waste **2010**, 339–339 (2010). https://doi.org/10.1201/b10569-42
11. Cenovus Energy, *Oil Sands, Water Management*, (2016) 2014–2015. http://www.cenovus.com/operations/oilsands.html.
12. A. Energy, Steam Assisted Gravity Drainage Facts and Stats Steam Assisted Gravity Drainage Process, (2017) 2017. https://open.alberta.ca/dataset/f7c779ea-9776-4d59-a1b3-178d533f0ebc/resource/aac73d46-3ae0-478e-9b19-e64afa41b1f2/download/FSSAGD.pdf.
13. M. Rashedi, O. Xu, S. Kwak, S. Sedghi, J. Liu, B. Huang, An integrated first principle modeling to steam assisted gravity drainage (SAGD). J. Pet. Sci. Eng. **163**, 501–510 (2018). https://doi.org/10.1016/j.petrol.2018.01.005
14. L. Guangyue, L. Shangqi, S. Pingping, L. Yang, L. Yanyan, A new optimization method for steam-liquid level intelligent control model in oil sands Steam-assisted Gravity

Drainage (SAGD) process. Pet. Explor. Dev. **43**, 301–307 (2016). https://doi.org/10.1016/S1876-3804(16)30034-9
15. A. Al-As'ad, *Treatment of SAGD Water Using Low Coagulant Dose And Fenton Oxidation*, MCs Thesis, Univeristy of Calgary, (2013).
16. X. Dong, H. Liu, Z. Zhang, L. Wang, Z. Chen, Performance of multiple thermal fluids assisted gravity drainage process in Post SAGD Reservoirs. J. Pet. Sci. Eng. **154**, 528–536 (2017). https://doi.org/10.1016/j.petrol.2016.12.032
17. J. Hajinasiri, *Treatment of Steam Assisted Gravity Drainage Produced Water Using Polymeric Membranes*, MSc Thesis, University of Alberta, (2015).
18. M.A. Petersen, H. Grade, Analysis of steam assisted gravity drainage produced water using two-dimensional gas chromatography with time-of-flight mass spectrometry. Ind. Eng. Chem. Res. **50**, 12217–12224 (2011). https://doi.org/10.1021/ie200531h
19. N.A. Abdelwahab, N. Shukry, S.F. El-kalyoubi, Separation of Emulsified Oil from Wastewater Using Polystyrene and Surfactant Modified Sugarcane Bagasse Wastes Blend. Clean Techn. Environ. Policy **23**, 235–249 (2020). https://doi.org/10.1016/j.seppur.2008.06.002
20. Y. Gang, C. Shuo, Q. Xie, W. Gaoliang, F. Xinfei, Y. Hongtao, Enhanced separation performance of carbon nanotube–polyvinyl alcohol composite membranes for emulsified oily wastewater treatment under electrical assistance. Sep. Purif. Technol. **197**, 107–115 (2018). https://doi.org/10.1016/j.seppur.2008.12.015
21. S.S. Atallah, C. Tremblay, A.Y. Mortazavi, Silane surface modified ceramic membranes for the treatment and recycling of SAGD produced water. J. Pet. Sci. Eng. **157**, 349–358 (2017). https://doi.org/10.2118/04-08-01
22. T. Kar, A. Mukhametshina, Y. Unal, B. Hascakir, The effect of clay type on steam-assisted-gravity-drainage performance. J. Can. Pet. Technol. **54**, 412–423 (2015). https://doi.org/10.2118/173795-PA%0A
23. K. Zhang, D. Pernitsky, M. Jafari, Q. Lu, Effect of MgO slaking on silica removal during warm lime softening of sagd produced water. Ind. Eng. Chem. Res. **60**, 1839–1849 (2021). https://doi.org/10.2118/97686-MS
24. H. Kawaguchi, Z. Li, Y. Masuda, K. Sato, H. Nakagawa, Dissolved organic compounds in reused process water for steam-assisted gravity drainage oil sands extraction. Water Res. **46**, 5566–5574 (2012). https://doi.org/10.1016/j.watres.2012.07.036
25. E.W. Allen, Process water treatment in canada's oil sands industry: II. A review of emerging technologies. J. Environ. Eng. Sci. **7**, 499–524 (2008)
26. A.T. Lima, K. Mitchell, D.W.O. Connell, J. Verhoeven, P. Van Cappellen, Environmental science & policy the legacy of surface mining : remediation , restoration , reclamation and rehabilitation. Environ Sci Policy **66**, 227–233 (2016). https://doi.org/10.1016/j.envsci.2016.07.011
27. J.Z. Zhou, H. Li, R.S. Chow, Q. Liu, Z. Xu, J. Masliyah, Role of mineral flotation technology in improving bitumen extraction from mined Athabasca oil sands—II. Flotation hydrodynamics of water-based oil sand extraction. Can. J. Chem. Eng. **98**, 330–352 (2020). https://doi.org/10.1002/cjce.23598
28. C.E. Willis, V.L.S. Louis, J.L. Kirk, K.A.S. Pierre, C. Dodge, Tailings ponds of the Athabasca Oil Sands Region, Alberta, Canada, are likely not significant sources of total mercury and methylmercury to nearby ground and surface waters. Sci. Total Environ. **647**, 1604–1610 (2019). https://doi.org/10.1016/j.scitotenv.2018.08.083
29. S. Shamim, Novel Mature Fine Tailings Treatment Using Colloidal Silica Particles, (2018).
30. M.E. Hansen, E. Dursteler, Pipeline, rail & trucks: economic, environmental, and safety impacts of transporting oil and gas in the U.S, Strata. (2017) 1–6. https://www.strata.org/pdf/2017/pipelines.pdf.
31. https://www.capp.ca/energy/transportation/, (n.d.).
32. J. Beyer, H.C. Trannum, T. Bakke, P.V. Hodson, T.K. Collier, Environmental effects of the deepwater horizon oil spill: a review. Mar. Pollut. Bull. **110**, 28–51 (2016). https://doi.org/10.1016/j.marpolbul.2016.06.027

33. A.Y. Ku, C.S. Henderson, M.A. Petersen, D.J. Pernitsky, A.Q. Sun, Aging of water from Steam-Assisted Gravity Drainage (SAGD) operations due to air exposure and effects on ceramic membrane filtration. Ind. Eng. Chem. Res. **51**, 7170–7176 (2012). https://doi.org/10.1021/ie3005513
34. G.T. John, C. Crittenden, R. Rhodes Trussell, D.W. Hand, K.J. Howe, *Water Treatment Princible and Design*, 2nd edn. (Willy, 2005)
35. M. Drahansky, M. Paridah, A. Moradbak, A. Mohamed, F.A. Owolabi, M. Asniza, S.H. Abdul Khalid, Aqueous Silica and Silica Polymerisation. INTECH **3**, 13 (2016). https://doi.org/10.5772/57353
36. D.B. van den Heuvel, E. Gunnlaugsson, I. Gunnarsson, T.M. Stawski, C.L. Peacock, L.G. Benning, Understanding amorphous silica scaling under well-constrained conditions inside geothermal pipelines. Geothermics **76**, 231–241 (2018)
37. Z. Yubin, Z. AXuelu, Removal of silica from heavy oil wastewater to be reused in a boiler by combining magnesium and zinc compounds with coagulation. Desalination **216**, 147–159 (2007)
38. Z. Yubin, Y. Changzhu, P. Wenhong, Z. Xuelu, Removal of silica from heavy oil wastewater to be reused in a boiler by combining magnesium and zinc compounds with coagulation. Desalination **216**, 147–159 (2007)
39. C. Héline, L.-T. Anh, Effective removal of silica and sulfide from oil sands thermal in-situ produced water by electrocoagulation. J. Hazard. Mater. **380**, 120880 (2019)
40. K. Zhang, D. Pernitsky, M. Jafari, Q. Lu, Effect of MgO slaking on silica removal during warm lime softening of SAGD produced water. Ind. Eng. Chem. Res. (2021). https://doi.org/10.1021/acs.iecr.0c05484
41. I. Latour, R. Miranda, A. Blanco, Silica removal with sparingly soluble magnesium compounds. Part I. Sep. Purif. Technol. **138**, 210–218 (2014). https://doi.org/10.1016/j.seppur.2014.10.016
42. A. Charbel, S.Y. Tremblaya, A. Mortazavi, Silane surface modified ceramic membranes for the treatment and recycling of SAGD produced water. J. Pet. Sci. Eng. **157**, 349–358 (2017)
43. B. Khorshidi, I. Biswas, T. Ghosh, T. Thundat, M. Sadrzadeh, Robust fabrication of thin film polyamide-TiO2 nanocomposite membranes with enhanced thermal stability and anti-biofouling propensity. Sci. Rep. **8**, 1–10 (2018). https://doi.org/10.1038/s41598-017-18724-w
44. A. Karkooti, A.Z. Yazdi, P. Chen, M. McGregor, N. Nazemifard, M. Sadrzadeh, Development of advanced nanocomposite membranes using graphene nanoribbons and nanosheets for water treatment. J. Membr. Sci. **560**, 97–107 (2018). https://doi.org/10.1016/j.memsci.2018.04.034
45. C.H. Rawlins, F. Sadeghi, N.O. Varco, Experimental study on oil removal in nutshell filters for produced-water treatment. SPE Prod. Oper. **33**, 145–153 (2017)
46. T. Altun, E. Pehlivan, Removal of Cr(VI) from aqueous aolutions by modified walnut shells. Food Chem. **132**, 693–700 (2012). https://doi.org/10.1016/j.foodchem.2011.10.099
47. D. Ding, Z. Lei, Y. Yang, C. Feng, Z. Zhang, Selective removal of cesium from aqueous solutions with Nickel (II) Hexacyanoferrate (III) functionalized agricultural residue-walnut shell. J. Hazard. Mater. **270**, 187–195 (2014). https://doi.org/10.1016/j.jhazmat.2014.01.056
48. M. Zhu, J. Yao, L. Dong, J. Sun, Adsorption of Naphthalene from aqueous solution onto fatty acid modified walnut shells. Chemosphere **144**, 1639–1645 (2016). https://doi.org/10.1016/j.chemosphere.2015.10.050
49. S. Li, Z. Zeng, W. Xue, Adsorption of lead ion from aqueous solution by modified walnut shell: kinetics and thermodynamics. Environ. Technol. (United Kingdom). **40**, 1810–1820 (2019). https://doi.org/10.1080/09593330.2018.1430172
50. Q. Yu, M. Li, P. Ning, H. Yi, X. Tang, Characterization of metal oxide-modified walnut-shell activated carbon and its application for phosphine adsorption: equilibrium, regeneration, and mechanism studies. J. Wuhan Univ. Technol. Mater. Sci. Ed. **34**, 487–495 (2019). https://doi.org/10.1007/s11595-019-2078-y
51. A. Hethnawi, K. Hashlamoun, S. Sessarego, M. Chehelamirani, N.N. Nassar, Simultaneous removal of Silica and TOC from Steam Assisted Gravity Drainage (SAGD) produced

water using iron-hydroxide-coated walnut shell filter media. J. Water Process Eng. JWPE-D-20 (2021)
52. L. Shamaei, B. Khorshidi, B. Perdicakis, M. Sadrzadeh, Treatment of oil sands produced water using combined electrocoagulation and chemical coagulation techniques. Sci. Total Environ. **645**, 560–572 (2018). https://doi.org/10.1016/j.scitotenv.2018.06.387
53. B. Khorshidi, A. Bhinder, T. Thundat, D. Pernitsky, M. Sadrzadeh, Developing high throughput thin film composite polyamide membranes for forward osmosis treatment of SAGD produced water. J. Membr. Sci. **511**, 29–39 (2016). https://doi.org/10.1016/j.memsci.2016.03.052
54. A. Charbel, S.Y. Tremblaya, A. Mortazavi, Silane surface modified ceramic membranes for the treatment and recycling of SAGD produced water. J. Pet. Sci. Eng. **157**, 349–358 (2017). https://doi.org/10.1016/j.petrol.2017.07.007
55. C. Atallah, S. Mortazavi, A.Y. Tremblay, A. Doiron, Surface-modified multi-lumen tubular membranes for SAGD-produced water treatment. Energy Fuel **33**, 5766–5776 (2019). https://doi.org/10.1021/acs.energyfuels.9b00585
56. L. Shamaei, B. Khorshidi, M.A. Islam, M. Sadrzadeh, Development of antifouling membranes using agro-industrial waste lignin for the treatment of Canada's oil sands produced water. J. Membr. Sci. **611**, 118326 (2020). https://doi.org/10.1016/j.memsci.2020.118326
57. A. El-Qanni, *Development of Sustainable Nanosorbcats Based Technology for Hydrocarbons and Organic Pollutants Recovery from Industrial Wastewater*, (2017)
58. A. Hethnawi, *Poly(ethylenimine)-Functionalized Pyroxene Nanoparticles Embedded on Diatomite for Removal of Total Organic Carbon from Industrial Wastewater: Batch and Fixed-bed studies* (University of Calgary, 2017)
59. R. Thummar, N. Limbasiya, A. Upadhyay, *Wet Air Oxidation Process for Sludge Treatment* (Zimpro Process), Semant. Sch. Corpus ID: (2015).
60. P. Haghighat, L.C. Ortega, P. Pereira-Almao, Experimental study on catalytic hydroprocessing of solubilized asphaltene in water: A proof of concept to upgrade asphaltene in the aqueous phase. Energy Fuel **30**, 2904–2918 (2016). https://doi.org/10.1021/acs.energyfuels.6b00275
61. A.D. Manasrah, N.N. Nassar, L.C. Ortega, Conversion of petroleum coke into valuable products using oxy-cracking technique. Fuel **215**, 865–878 (2018). https://doi.org/10.1016/j.fuel.2017.11.103
62. A.D. Manasrah, G. Vitale, N.N. Nassar, Catalytic oxy-cracking of petroleum coke on copper silicate for production of humic acids. Appl. Catal. B Environ. **264**, 118472 (2020). https://doi.org/10.1016/j.apcatb.2019.118472
63. L. Li, P. Chen, E.F. Gloyna, Generalized kinetic model for wet oxidation of organic compounds. AICHE J. **37**, 1687–1697 (1991). https://doi.org/10.1002/aic.690371112
64. A.D. Manasrah, N.N. Nassar, L.C. Ortega, Conversion of petroleum coke into valuable products using oxy-cracking technique. Fuel **215**, 865–878 (2018)
65. G. Nafie, A. D. Manasrah, B. Mackay, I. Badran, N. N. Nassar (eds.), Oxy-cracking reaction for enhanced settling and dewaterability of oil sands tailings. Ind. Eng. Chem. Res. **58**, 4988–4996 (2019)
66. A.D. Manasrah, N.N. Nassar, Oxy-cracking technique for producing non-combustion products from residual feedstocks and cleaning up wastewater. Appl. Energy **280**, 115890 (2020). https://doi.org/10.1016/j.apenergy.2020.115890
67. A. Hethnawi, N.N. Nassar, A.D. Manasrah, G. Vitale, Polyethylenimine-functionalized pyroxene nanoparticles embedded on diatomite for adsorptive removal of dye from textile wastewater in a fixed-bed column. Chem. Eng. J. **320**, 389–404 (2017). https://doi.org/10.1016/j.cej.2017.03.057
68. R.M. Cornell, U. Schwertmann, the Iron Oxides: Structure, Properties, Reactions, Occurrences and Uses, 2nd ed., Copyright © 2003 Wiley-VCH Verlag GmbH & Co. KGaA, (2003). doi:https://doi.org/10.1002/3527602097.
69. C. Nieto-Delgado, J.R. Rangel-Mendez, Anchorage of Iron Hydro (oxide) Nanoparticles onto Activated Carbon to Remove As (V) from Water. Water Res. **46**, 2973–2982 (2012)

70. J. Zhao, Z. Lu, X. He, X. Zhang, Q. Li, T. Xia, W. Zhang, C. Lu, Y. Deng, One-Step Fabrication of Fe(OH)3@Cellulose Hollow Nanofibers with Superior Capability for Water Purification. ACS Appl. Mater. Interfaces **9**, 25339–25349 (2017). https://doi.org/10.1021/acsami.7b07038
71. X. Zhu, L. Yiming, H. Yang, Z. Yangge, S. Changxing, W. Weiqing, Adsorption of Ferric Ions on the Surface of Bastnaesite and Its Significance in Flotation. Miner. Eng. **158**, 106588 (2020)
72. S. Grimme, S. Ehrlich, L. Goerigk, Effect of the damping function in dispersion corrected density functional theory. J. Comput. Chem. **32**, 1456–1465 (2011)
73. S. Grimme, J. Antony, S. Ehrlich, H. Krieg, A consistent and accurate ab initio parametrization of density functional dispersion correction (DFT-D) for The 94 Elements H-Pu. J. Chem. Phys. **132**, 154104 (2010)
74. P.E. Blöchl, Projector Augmented-wave method. Phys. Rev. B **50**, 17953 (1994)
75. R.G. Pillai, N. Yang, S. Thi, J. Fatema, M. Sadrzadeh, D. Pernitsky, Characterization and comparison of dissolved organic matter signatures in steam-assisted gravity drainage process water samples from athabasca oil sands. Energy Fuel **31**, 8363–8373 (2017)
76. S. Guha Thakurta, A. Maiti, D.J. Pernitsky, S. Bhattacharjee, Dissolved organic matter in steam assisted gravity drainage boiler blow-down water. Energy Fuel **27**, 3883–3890 (2013)
77. Y. Nishiyama, P. Langan, H. Chanzy, Crystal structure and hydrogen-bonding system in cellulose Iβ from SYNCHROTRON X-ray and neutron fiber diffraction. J. Am. Chem. Soc. **124**, 9074–9082 (2002)
78. C. Zhu, I. Dobryden, J. Rydén, S. Öberg, A. Holmgren, A.P. Mathew, Adsorption behavior of cellulose and its derivatives toward Ag (I) in aqueous medium: an AFM, spectroscopic, and DFT study. Langmuir **31**, 12390–12400 (2015)
79. D. Zheng, Y. Zhang, Y. Guo, J. Yue, Isolation and characterization of Nanocellulose with a Novel Shape from Walnut (Juglans regia L.) Shell agricultural waste. Polymers (Basel) **11**, 1130 (2019)
80. S. Zhao, J. Niu, L. Yun, K. Liu, S. Wang, J. Wen, Z. Zhang, The relationship among the structural, cellular, and physical properties of walnut shells. HortScience **54**, 275–281 (2019)
81. K. Momma, F. Izumi, VESTA 3 for three-dimensional visualization of crystal, volumetric and morphology data. J. Appl. Crystallogr. **44**, 1272–1276 (2011)
82. T. Tsuneda, *Density Functional Theory in Quantum Chemistry*, 3rd edn. (2014)
83. V. Vajihinejad, R. Guillermo, J.B.P. Soares, Dewatering Oil Sands Mature Fine Tailings (MFTs) with Poly(acrylamide-co-diallyldimethylammonium chloride): Effect of Average Molecular Weight and Copolymer Composition. Ind. Eng. Chem. Res. **56**, 1256–1266 (2017). https://doi.org/10.1021/acs.iecr.6b04348
84. R. Hripko, V. Vajihinejad, F. LopesMotta, J.B.P. Soares, Enhanced flocculation of oil sands mature fine tailings using hydrophobically modified polyacrylamide copolymers. Glob. Challenges. **2**, 1700135 (2018). https://doi.org/10.1002/gch2.201700135
85. S.P. Gumfekar, T.R. Rooney, R.A. Hutchinson, J.B.P. Soares, Dewatering oil sands tailings with degradable polymer flocculants. ACS Appl. Mater. Interfaces **9**, 36290–36300 (2017). https://doi.org/10.1021/acsami.7b10302
86. D.K. Thompson, F.L. Motta, J.B.P. Soares, Investigation on the flocculation of oil sands mature fine tailings with alkoxysilanes. Miner. Eng. **111**, 90–99 (2017). https://doi.org/10.1016/j.mineng.2017.06.008
87. C. Wang, D. Harbottle, Q. Liu, Z. Xu, Current state of fine mineral tailings treatment: a critical review on theory and practice. Miner. Eng. **58**, 113–131 (2014). https://doi.org/10.1016/j.mineng.2014.01.018
88. S. Renault, C. Lait, J.J. Zwiazek, M. MacKinnon, Effect of high salinity tailings waters produced from gypsum treatment of oil sands tailings on plants of the boreal forest. Environ. Pollut. **102**, 177–184 (1998). https://doi.org/10.1016/s0269-7491(98)00099-2

89. M.J. Salloum, M.J. Dudas, P.M. Fedorak, Microbial reduction of amended sulfate in anaerobic mature fine tailings from oil sand. Waste Manag. Res. **20**, 162–171 (2002). https://doi.org/10.1177/0734242X0202000208
90. J.G. Matthews, W.H. Shaw, M.D. Mackinnon, R.G. Cuddy, Development of composite tailings technology at Syncrude. Int. J. Surf. Min. Reclam. Environ. **16**, 24–39 (2002). https://doi.org/10.1076/ijsm.16.1.24.3407
91. D. Zhang, T. Thundat, R. Narain, Flocculation and dewatering of mature fine tailings using temperature-responsive cationic polymers. Langmuir **33**, 5900–5909 (2017). https://doi.org/10.1021/acs.langmuir.7b01160
92. L.G. Reis, R.S. Oliveira, T.N. Palhares, L.S. Spinelli, E.F. Lucas, D.R.L. Vedoy, E. Asare, J.B.P. Soares, Using acrylamide/propylene oxide copolymers to dewater and densify mature fine tailings. Miner. Eng. **95**, 29–39 (2016). https://doi.org/10.1016/j.mineng.2016.06.005
93. K.C. Lister, H. Kaminsky, R.A. Hutchinson, Evaluation of a novel polymeric flocculant for enhanced water recovery of mature fine tailings. Processes. **8**, 735 (2020). https://doi.org/10.3390/pr8060735
94. D.R. Vedoy, J.B. Soares, Water-soluble polymers for oil sands tailing treatment: A Review. Can. J. Chem. Eng. **93**, 888–904 (2015)
95. A. Alamgir, D. Harbottle, J. Masliyah, Z. Xu, Al-PAM assisted filtration system for abatement of mature fine tailings. Chem. Eng. Sci. **80**, 91–99 (2012). https://doi.org/10.1016/j.ces.2012.06.010
96. W.Y. Yang, J.W. Qian, Z.Q. Shen, A novel flocculant of Al(OH)3-polyacrylamide ionic hybrid. J. Colloid Interface Sci. **273**, 400–405 (2004). https://doi.org/10.1016/j.jcis.2004.02.002
97. X. Wei, J. Tao, M. Li, B. Zhu, X. Li, Z. Ma, T. Zhao, B. Wang, B. Suo, H. Wang, J. Yang, L. Ye, X. Qi, Polyacrylamide-based inorganic hybrid flocculants with self-degradable property. Mater. Chem. Phys. **192**, 72–77 (2017). https://doi.org/10.1016/j.matchemphys.2017.01.064
98. K.E. Lee, T.T. Teng, N. Morad, B.T. Poh, Y.F. Hong, Flocculation of kaolin in water using novel calcium chloride-polyacrylamide (CaCl2-PAM) hybrid polymer. Sep. Purif. Technol. **75**, 346–351 (2010). https://doi.org/10.1016/j.seppur.2010.09.003
99. H. Lu, Y. Wang, L. Li, Y. Kotsuchibashi, R. Narain, H. Zeng, Temperature- and pH-responsive benzoboroxole-based polymers for flocculation and enhanced dewatering of fine particle suspensions. ACS Appl. Mater. Interfaces **7**, 27176–27187 (2015). https://doi.org/10.1021/acsami.5b09874
100. L. Botha, S. Davey, B. Nguyen, A.K. Swarnakar, E. Rivard, J.B.P. Soares, Flocculation of oil sands tailings by hyperbranched functionalized polyethylenes (HBfPE). Miner. Eng. **108**, 71–82 (2017). https://doi.org/10.1016/j.mineng.2017.02.004
101. G. Nafie, G. Vitale, L. Carbognani Ortega, N.N. Nassar, Nanopyroxene grafting with β-Cyclodextrin monomer for wastewater applications. ACS Appl. Mater. Interfaces **9**, 42393–42407 (2017). https://doi.org/10.1021/acsami.7b13677
102. J. Roberts, M. Caserio, *Basic Principles of Organic Chemistry*, 2nd edn. (Benjamin, 1977)
103. A. Kumar, G. Sharma, M. Naushad, S. Thakur, SPION/β-cyclodextrin core-shell nanostructures for oil spill remediation and organic pollutant removal from waste water. Chem. Eng. J. **280**, 175–187 (2015). https://doi.org/10.1016/j.cej.2015.05.126
104. B. Doshi, M. Sillanpää, S. Kalliola, A review of bio-based materials for oil spill treatment. Water Res. **135**, 262–277 (2018). https://doi.org/10.1016/j.watres.2018.02.034
105. J. Ge, H.Y. Zhao, H.W. Zhu, J. Huang, L.A. Shi, S.H. Yu, Advanced sorbents for oil-spill cleanup: recent advances and future perspectives. Adv. Mater. **28**, 10459–10490 (2016). https://doi.org/10.1002/adma.201601812
106. M. Husseien, A.A. Amer, A. El-Maghraby, N. Hamedallah, Oil spill removal from water by using corn stalk: factors affecting sorption process. Int. J. Environ. Waste Manag. **16**, 281–292 (2015). https://doi.org/10.1504/IJEWM.2015.074907
107. M.O. Adebajo, R.L. Frost, J.T. Kloprogge, O. Carmody, S. Kokot, Porous materials for oil spill cleanup: a review of synthesis and absorbing properties. J. Porous. Mater. **10**, 159–170 (2003). https://doi.org/10.1023/A:1027484117065

108. M.F. Fingas, *Handbook of Oil Spill Science and Technology* (Wiley, 2015)
109. K.B. Debs, D.S. Cardona, H.D. da Silva, N.N. Nassar, E.N. Carrilho, P.S. Haddad, G. Labuto, Oil spill cleanup employing magnetite nanoparticles and yeast-based magnetic bionanocomposite. J. Environ. Manag. **230**, 405–412 (2019)
110. A. Bazargan, J. Tan, G. McKay, Standardization of oil sorbent performance testing. J. Test. Eval. **6**, 1271–1278 (2015)
111. J.H. Ramirez Leyva, A. Hethnawi, G. Vitale, N.N. Nassar, Magnetic nanostructured white graphene for oil spill and water cleaning. Ind. Eng. Chem. Res. **57**, 13065–13076 (2018). https://doi.org/10.1021/acs.iecr.8b02785
112. A. El-qanni, N.N. Nassar, G. Vitale, A. Hassan, Maghemite nanosorbcats for methylene blue adsorption and subsequent catalytic thermo-oxidative decomposition: computational modeling and thermodynamics studies. J. Colloid Interface Sci. **461**, 396–408 (2016). https://doi.org/10.1016/j.jcis.2015.09.041
113. O. Saber, N.H. Mohamed, A. Alijaafari, Synthesis of magnetic nanoparticles and nanosheets for oil spill removal. Nanosci. Nanotechnol-Asia **5**, 32–43 (2015)
114. A.A.S. Osama, H.M. Nermen, Synthesis of magnetic nanoparticles and nanosheets for oil spill removal. Nanosci Nanotechnol Asia **5**, 32–43 (2015)
115. T. Lü, Y. Chen, D. Qi, Z. Cao, D. Zhang, H. Zhao, Treatment of emulsified oil wastewaters by using chitosan grafted magnetic nanoparticles. J. Alloys Compd. **696**, 1205–1212 (2017). https://doi.org/10.1016/j.jallcom.2016.12.118
116. L. Yu, G. Hao, J. Gu, S. Zhou, N. Zhang, W. Jiang, Fe3O4/PS magnetic nanoparticles: Synthesis, characterization and their application as sorbents of oil from waste water. J. Magn. Magn. Mater. **394**, 14–21 (2015). https://doi.org/10.1016/j.jmmm.2015.06.045
117. X. Gui, Z. Zeng, Z. Lin, Q. Gan, R. Xiang, Y. Zhu, A. Cao, Z. Tang, Magnetic and highly recyclable macroporous carbon nanotubes for spilled oil sorption and separation. ACS Appl. Mater. Interfaces **5**, 5845–5850 (2013). https://doi.org/10.1021/am4015007
118. W. Ngarmkam, C. Sirisathitkul, C. Phalakornkule, Magnetic composite prepared from palm shell-based carbon and application for recovery of residual oil from POME. J. Environ. Manag. **92**, 472–479 (2011). https://doi.org/10.1016/j.jenvman.2010.08.031
119. J.H. Ramirez Leyva, A. Hethnawi, G. Vitale, N.N. Nassar, Magnetic nanostructured white graphene for oil spill and water cleaning. Ind. Eng. Chem. Res. **57**, 13065–13076 (2018). https://doi.org/10.1021/acs.iecr.8b02785
120. K.B. Debs, D.S. Cardona, H.D.T. da Silva, N.N. Nassar, E.N.V.M. Carrilho, P.S. Haddad, G. Labuto, Oil spill cleanup employing magnetite nanoparticles and yeast-based magnetic bionanocomposite. J. Environ. Manag. **230**, 405–412 (2019). https://doi.org/10.1016/j.jenvman.2018.09.094
121. P. Xu, G. Ming, D. Lian, C. Ling, S. Hu, M. Hua, Use of iron oxide nanomaterials in wastewater treatment : a review. Sci. Total Environ. **424**, 1–10 (2012). https://doi.org/10.1016/j.scitotenv.2012.02.023